

Figure 1

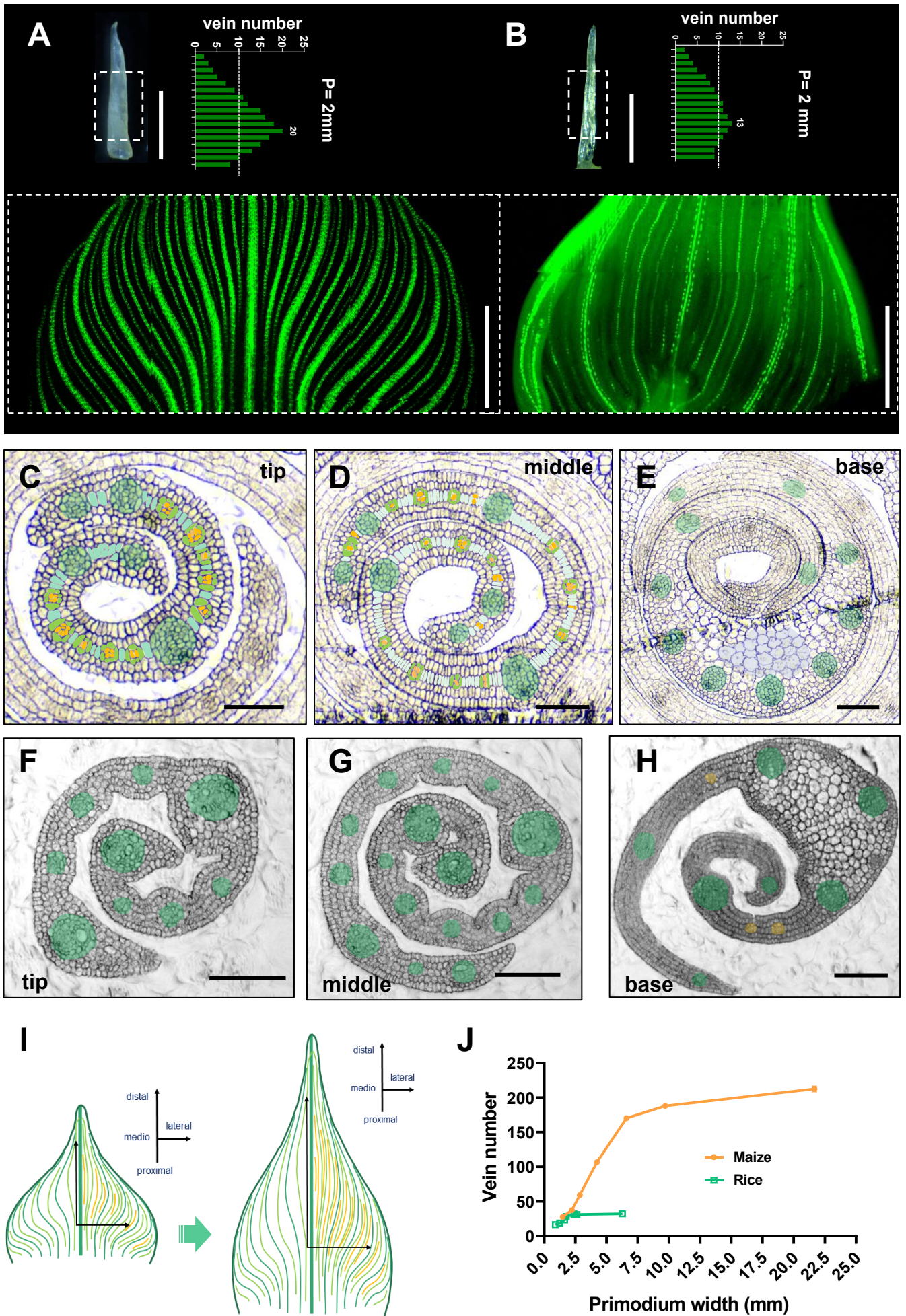


Figure 1. Analysis of vein development patterns in maize and rice leaf primordium.

A. Left: the maize primordium with longitudinal length of 2 mm. Scale bar: 1 mm. Right: Vein number distribution in maize leaf primordia from tip to base. Veins were counted from serial paraffin sections along tip-base axis (y-axis) and half of the number from each section (x-axis) were presented in the column charts. Bottom: confocal image showing pZmPIN1a::ZmPIN1a:YFP fluorescence marked developing veins in flattened maize leaf primordium. Scale bar: 465 μ m.

B. Left: the rice primordium with longitudinal length of 2 mm. Scale bar: 1 mm. Right: Vein number distribution in rice leaf primordia from tip to base. Veins were counted from serial paraffin sections and half of the number from each section were presented in the column charts. Bottom: Confocal image showing DR5::VENUS fluorescence marked developing veins in flattened rice leaf primordium. Scale bar: 200 μ m.

C-E. Transverse sections of the tip (C), middle (D), and base (E) of maize P4 leaf primordia highlighting the middle layer of ground tissue, which give rise to the procambial strands and intermediate veins (orange) and eventually lead to the differentiation of Kranz-type bundle sheath and mesophyll cells. The Kranz anatomy becomes evident in (C) with more developed bundle sheath and reduced number of mesophyll cells between veins, while in (D) multiple middle ground tissue cells or mesophyll precursors exist between veins, representing an actively developing stage of pre-Kranz anatomy. At the base section, parenchymal cells (light purple) next to the mid-rib are indicated. Scale bar: 60 μ m.

F-H. Transverse sections of the tip (F), middle (G), and base (H) of rice P3 leaf primordia (equivalent to maize P4 primordium in size). Proliferating veins in (H) are marked with orange color. Scale bar: 60 μ m.

I. Schematic depiction (according to unrolled and flattened samples) of vein formation and organization along with proximo–distal elongation and medio–lateral expansion of maize primordia, highlighting the recently and densely proliferated intermediate veins (marked in orange colour). Mid-rib and lateral veins are coloured dark green; older intermediate veins are coloured light green.

J. Vein number growing curves from primordia or leaves of different developmental stages of maize and rice. Vein numbers across the maximal primordium or leaf width were counted, from samples ranging from early primordia to expanded leaves. Error bars represent mean \pm SD ($n \geq 7$ biological replicates).

Fiaure 2

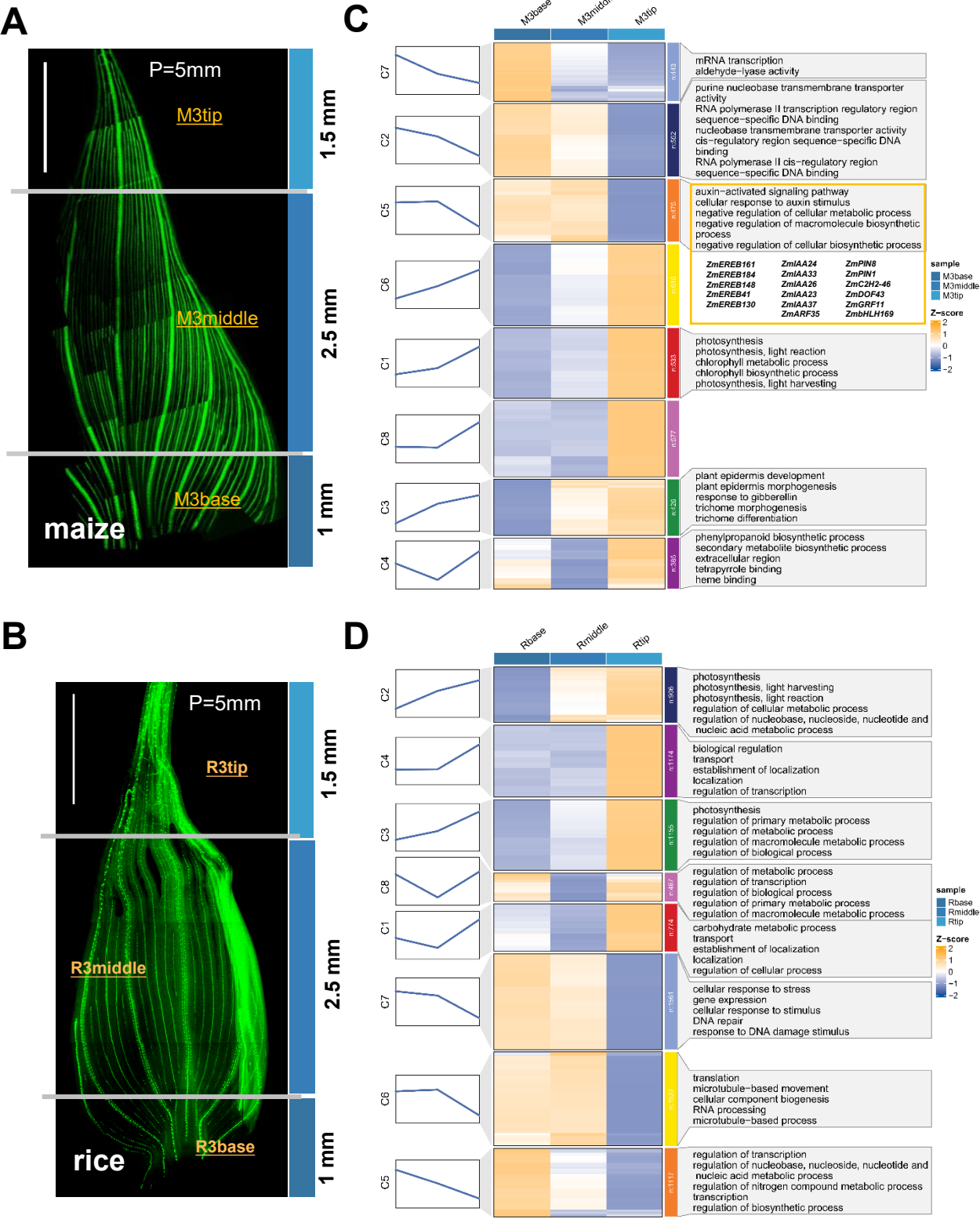


Figure 2. Bulk RNA-seq of segmented leaf primordia identifies enrichment of auxin related pathway.

A, B. Images indicating the 3 types of maize (A) or rice (B) tissues sampled for bulk RNA sequencing. The leaf primordium of about 5 mm were partitioned under dissection microscope into three parts: M/R3tip≈1.5 mm, M/R3middle≈2.5 mm, and M/R3base≈1 mm. Scale bar: 1000 μm. Note: Grey lines indicate the position where it was partitioned.

C, D. Differential gene expression analysis and functional enrichment were performed across three types of maize (C) or rice (D) tissues. C1–C8: On the left, a line plot displays the expression trends of differentially expressed genes (DEGs) within each cluster across all samples. The middle section presents a heatmap of DEG clusters in the three maize or rice tissue types. On the right, significantly enriched GO terms for DEGs in each cluster are shown following GO enrichment analysis. Note: The orange rectangle in (C) highlights transcription factors and auxin-related genes enriched in C5 of maize. The values were normalized using z-score method. The clustering method used was MFuzz, which defaults to using the weighted average as cluster centers.

Figure 3

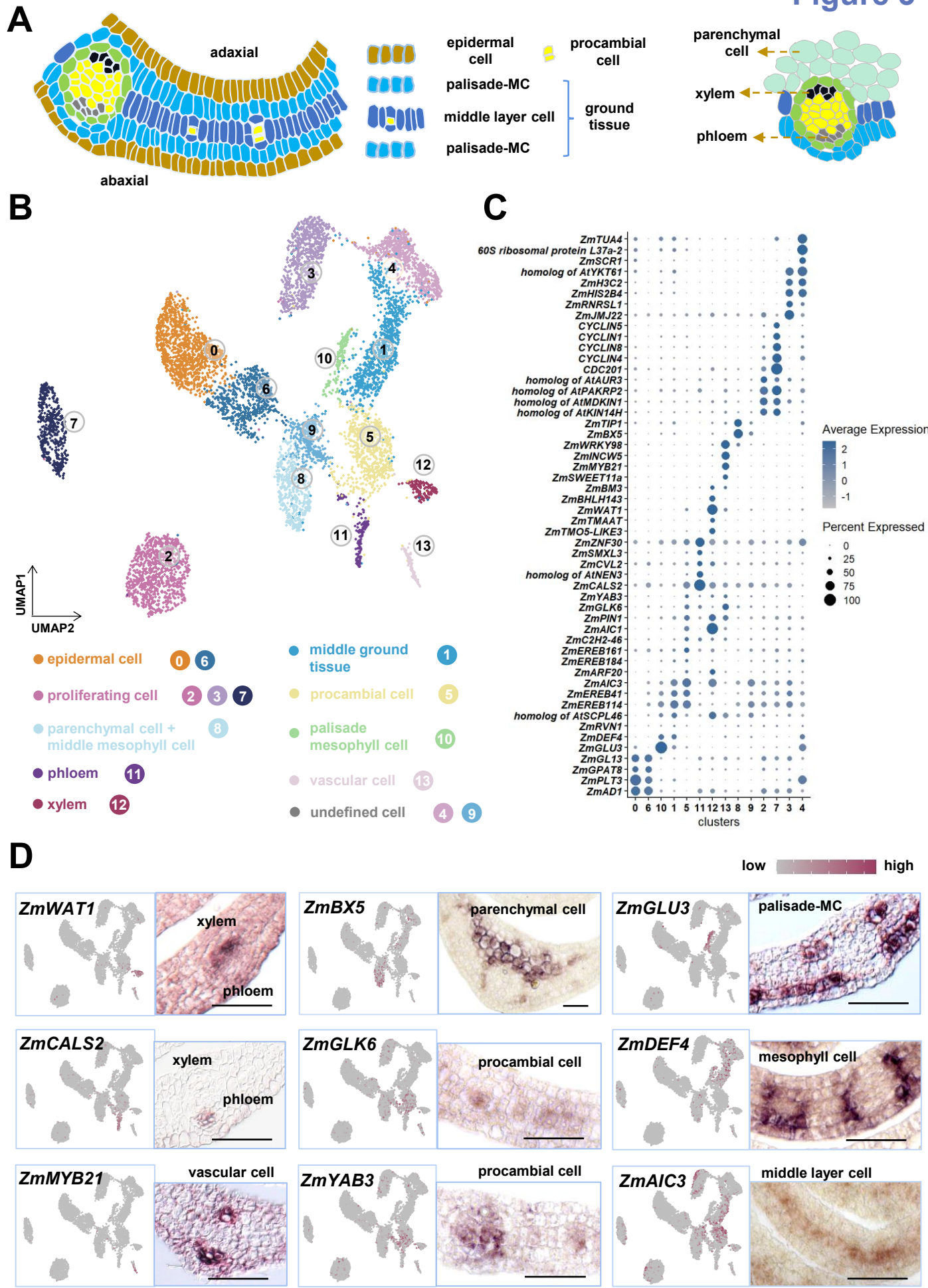


Figure 3. Cell heterogeneity in maize P4 leaf primordium.

A. Schematics of the anatomy and cell types representing a middle section of P4 leaf primordium. Cell clusters identified in (A) were indicated with related cell types in different colours.

B. Visualization of 14 cell clusters using UMAP. Dots, individual cells; $n = 7473$ cells; cell clusters are colored differently and labelled with circled numbers.

C. Expression patterns of representative cluster-specific marker genes. Dot color, the average expression level; Dot size, proportion of cluster cells expressing a given gene.

D. Expression pattern of representative cluster-enriched genes by UMAP plots and *in situ* hybridization among different cell type. The expressions in xylem, phloem, parenchymal cell, procambial cell, palisade-mesophyll cell, ground tissue and middle layer cells are shown. Scale bar, 50 μm .

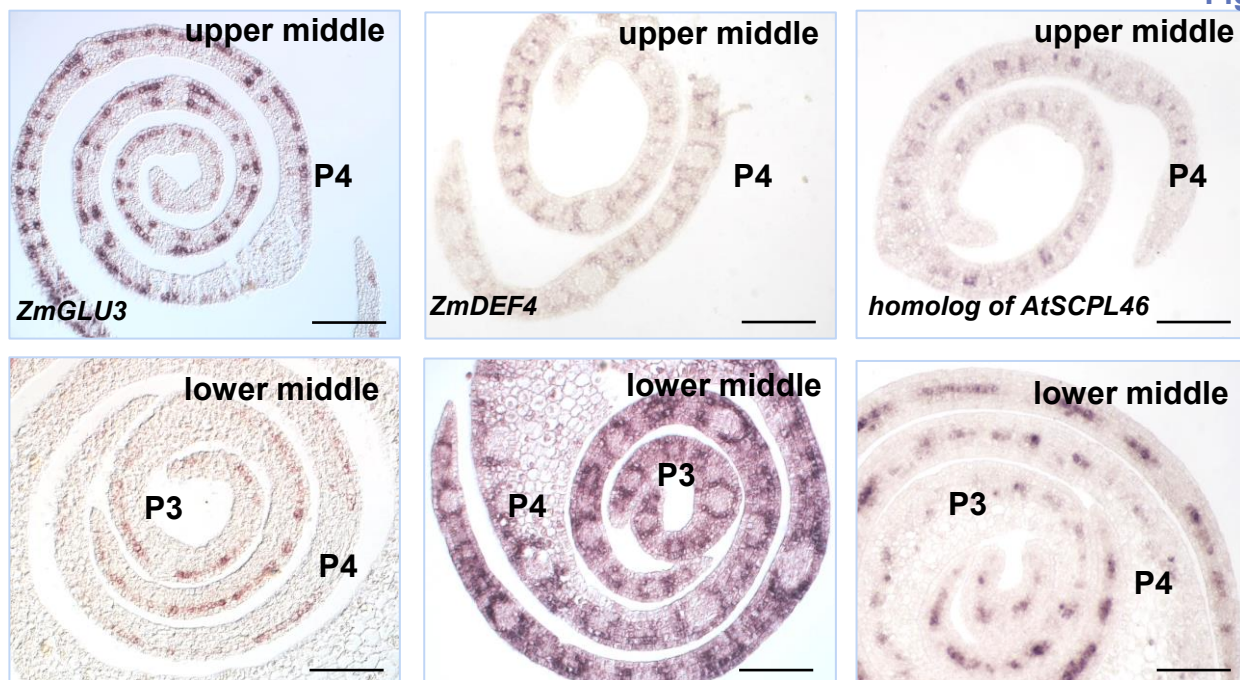
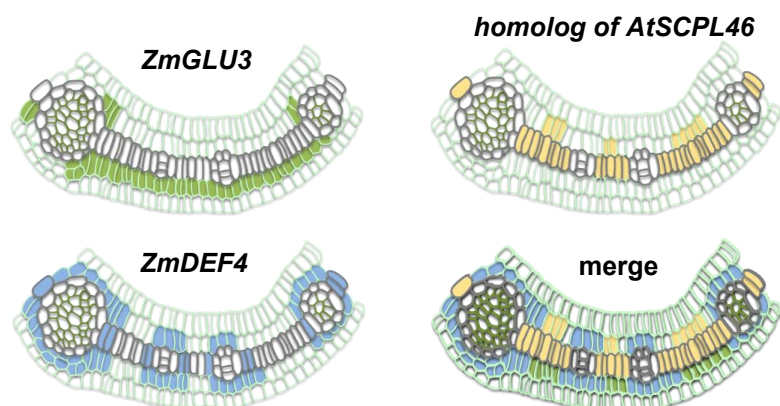
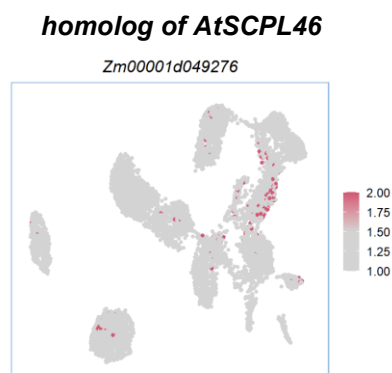
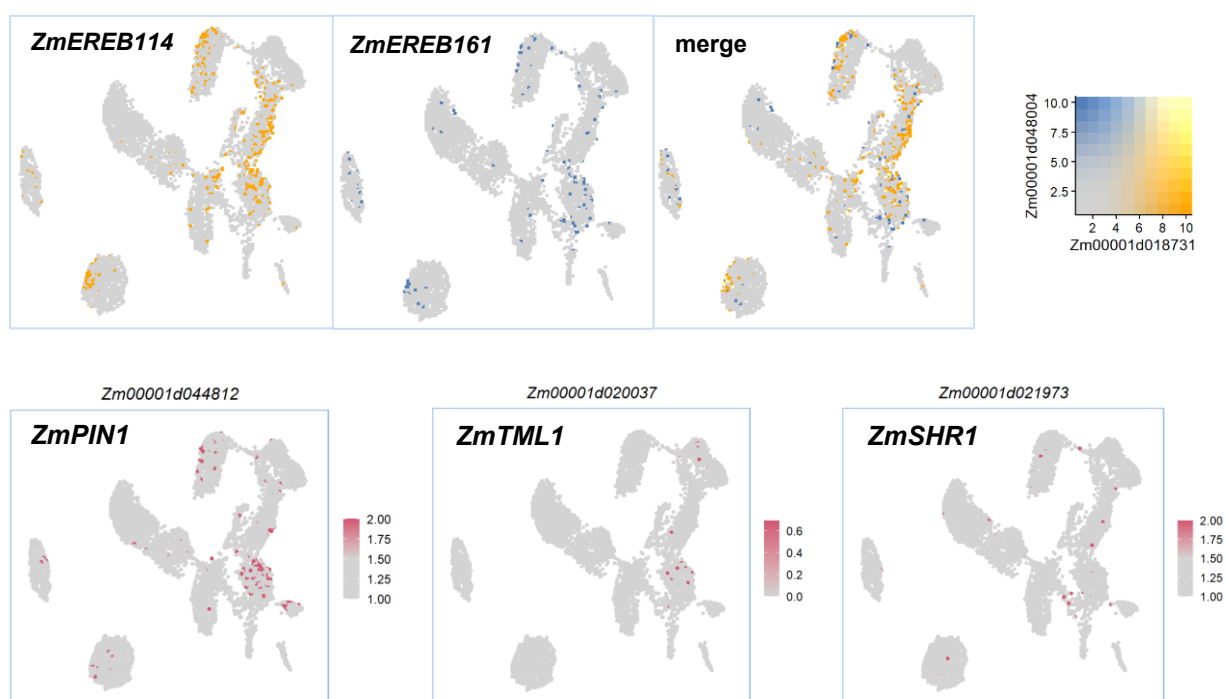
A**B****C****D**

Figure 4. Heterogeneity of ground tissue in maize P4 leaf primordium

A. *In situ* hybridization for the expression patterns of *ZmGLU3*, *ZmDEF4*, and *homolog of AtSCPL46* on upper middle and lower middle sections of maize P4 leaf primordium. Scale bar: 100 μ m.

B. Schematics of the expression patterns of *ZmGLU3*, *ZmDEF4*, and *homolog of AtSCPL46* on lower middle section. “Merged” shows the coverage of ground tissue by the expression of three genes.

C. Expression pattern of *homolog of AtSCPL46* by UMAP plots.

D. Expression pattern of *ZmPIN1*, *ZmTML1*, *ZmSHR1*, *ZmEREB114*, and *ZmEREB161* by UMAP plots.

Figure 5

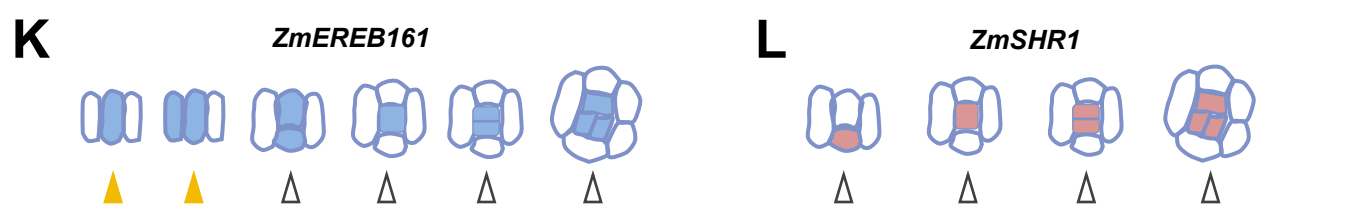
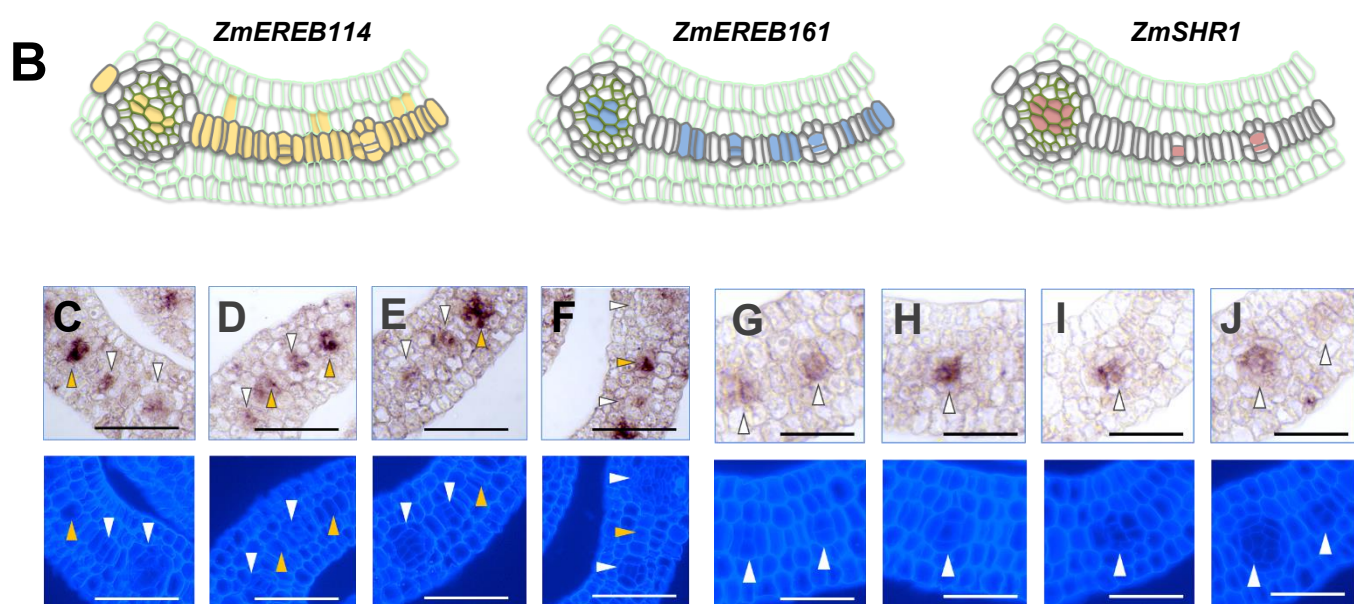
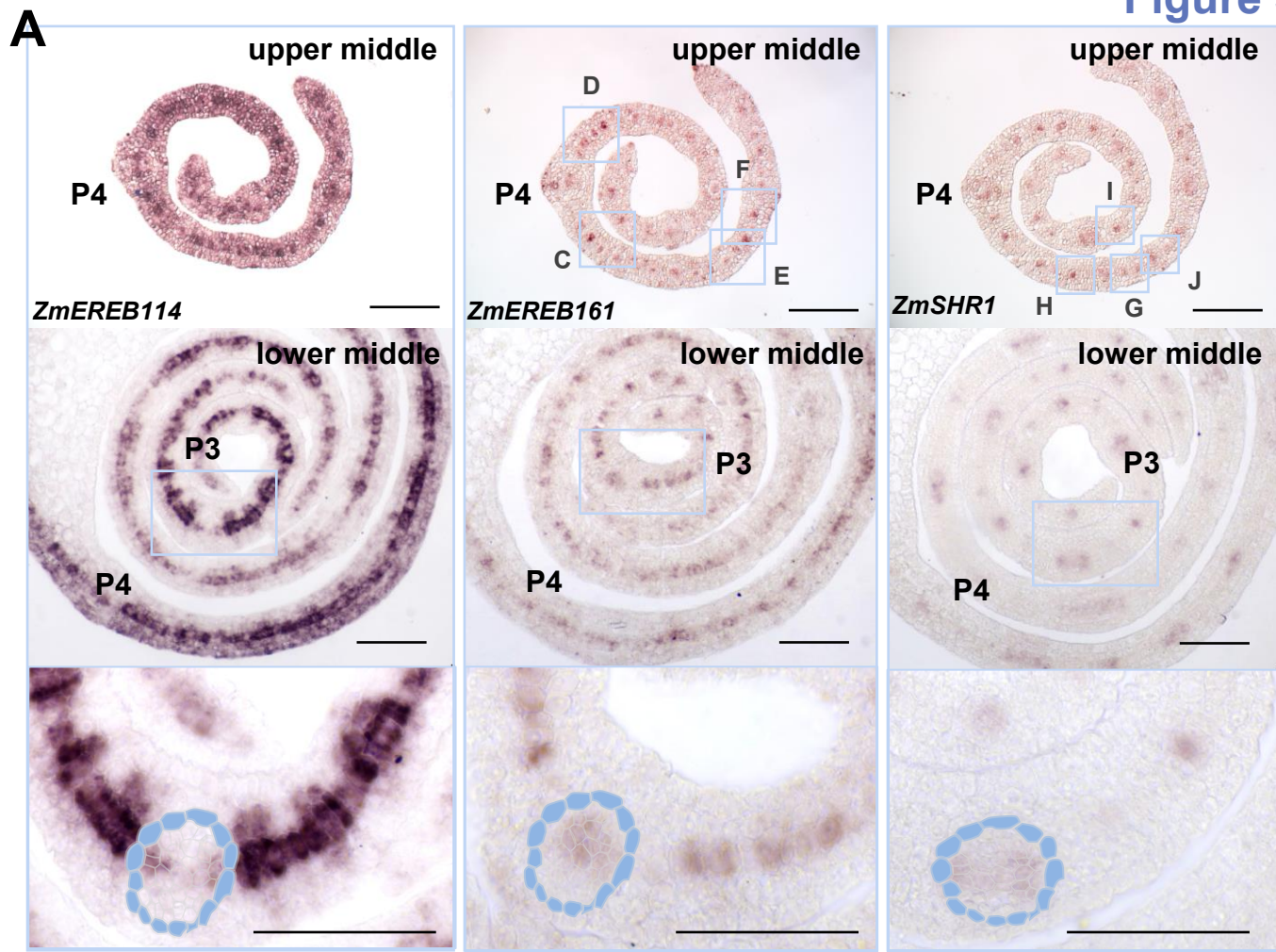


Figure 5. Heterogeneity of middle layer cell marked by *ZmEREBs* and *ZmSHR1*

A. *In situ* hybridization for the expression patterns of *ZmEREB114*, *ZmEREB161*, and *ZmSHR1* on upper middle and lower middle sections of maize P4 leaf primordium. Scale bar: 100 μm .

B. Schematics of the expression patterns of *ZmEREB114*, *ZmEREB161*, *ZmSHR1* on lower middle section.

C-F. Upper panel: Magnified images of the blue square framed regions from (A), showing *ZmEREB161* signals at different developmental stages of early Kranz anatomy; lower panel: UV activated fluorescent images of the corresponding regions from upper panel. Scale bar: 50 μm .

White arrow heads indicate the differentiating procambium (including those with the primary adaxial and abaxial precursors of BS cells, generated by the 1st and 2nd periclinal divisions of a single procambial initial cell); orange arrow heads indicate the potential single procambial initial cell (indicated by *in situ* hybridization signals) prior to periclinal division.

G-J. Upper panel: Magnified images of the blue square framed regions from (A), showing *ZmSHR1* signals at different developmental stages of early Kranz anatomy; lower panel: UV activated fluorescent images of the corresponding regions from upper panel. Scale bar: 30 μm .

K, L. Schematics of the expression patterns of *ZmEREB161* and *ZmSHR1* at single cell resolution.

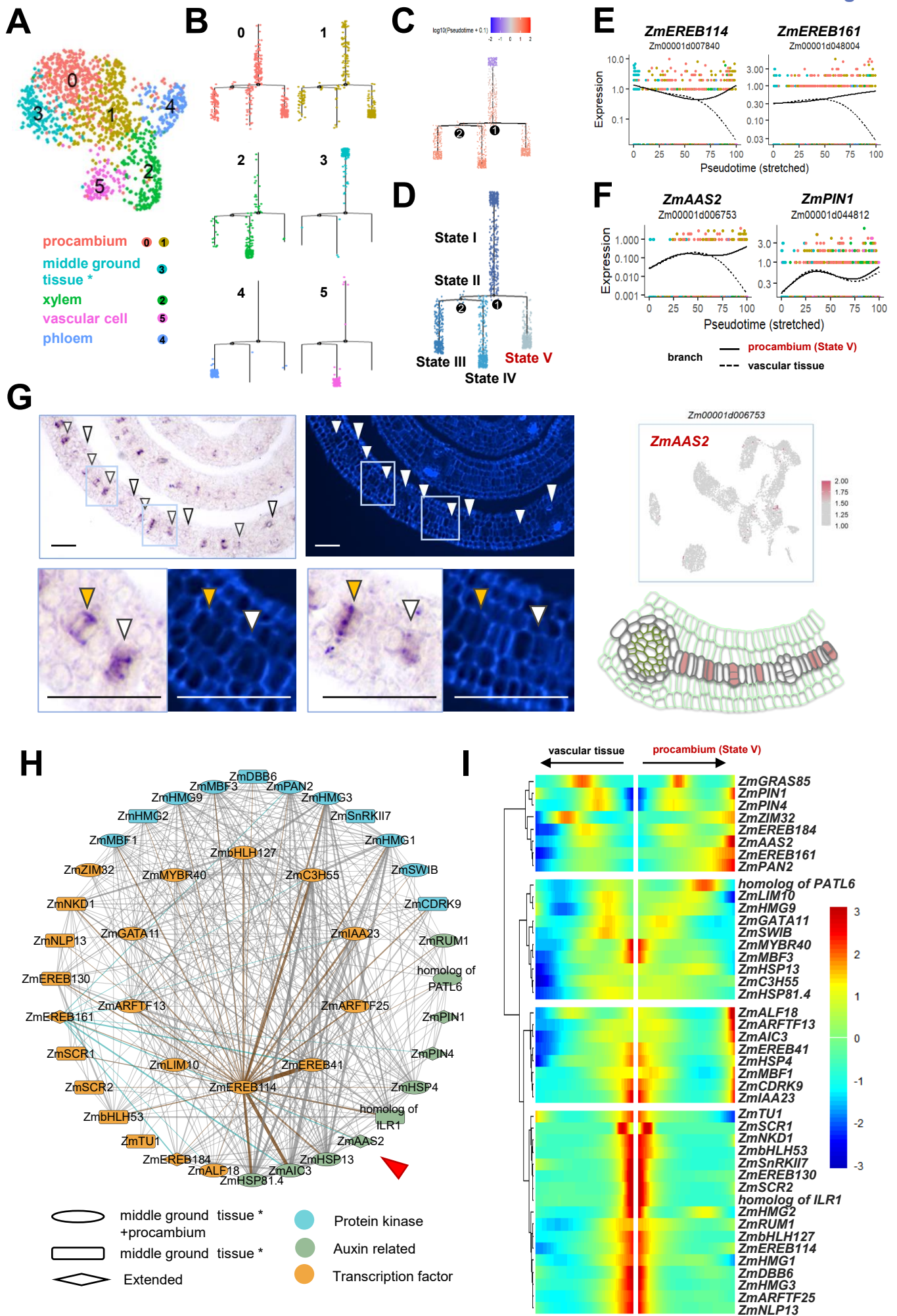


Figure 6. Differentiation trajectory of middle layer cell in maize P4 primordium identifies *ZmAAS2* and related network.

A. UMAP sub-clustering of the middle layer cell population (contain middle ground tissue, procambium, and vascular cells). Dots, individual cells; n = 1473 cells; cell clusters are colored differently and labelled with circled numbers. “middle ground tissue*” indicated a subset of cells obtained from the middle ground tissue (Cluster 1 in Figure 3A) expressing *ZmEREB114* and the homolog of *AtSCPL46*.

B-D. Pseudo-time analysis of differentiation trajectories in middle layer cell lineages performed using Monocle 2. The analysis identified five distinct differentiation states along the pseudo-time trajectory. The pseudo-temporal distribution of cell clusters revealed that “middle ground tissue*” (sub-cluster 3) and procambium cells (sub-clusters 0 and 1) were at the early stages of differentiation, gradually progressing into phloem (sub-cluster 4) and xylem (sub-cluster 2).

E. Kinetics plot showing relative expression of *ZmEREB114* and *ZmEREB161* along developmental pseudo-time splitting at “branch 1”. Solid lines indicate expression in “procambium (State V)”, while dotted lines represent vascular tissue expression.

F. Kinetics plot showing relative expression of the *ZmPIN1* and *ZmAAS2* along developmental pseudo-time splitting at “branch 1”. Solid lines indicate expression in “procambium (State V)”, while dotted lines represent vascular tissue expression. The abscissa represents the quasi-chronological order, and the ordinate represents the relative expression value of genes. The line denotes the smoothed average expression. The colored dots on the top shows the major cluster of contributing cells to the expression.

G. Upper panel: *In situ* hybridization for the transcript localization of *ZmAAS2* on lower middle transverse sections of maize P4 leaf primordium; lower panel: magnified images of the blue square framed regions and UV activated fluorescent images of the corresponding regions. Scale bar: 40 μ m. White arrow heads indicate the differentiating procambium; orange arrow heads indicate the potential single procambial initial cell prior to periclinal division.

Expression pattern of *ZmAAS2* by UMAP plot and schematics of the expression across transverse section are shown on the right.

H. Co-expression network of transcription factors (n=22), protein kinases (n=11), and auxin-related genes (n=10) enriched in the “middle ground tissue*” and procambium cells. Grey lines indicate co-expression connections inferred through network analysis, with line thickness representing correlation score. Brown lines show co-expression links between *ZmEREB114* and other genes, while cyan lines denote *ZmEREB161*-associated connections. Colors of nodes denote distinct gene type: orange for transcription factors, green for auxin-related genes, light blue for protein kinases. Node shapes denote different expression specificities. The inner circle highlights the top 10 hub transcription factors enriched in “middle ground tissue*” and procambium cells.

I. Pseudo-time trajectory heatmap by BEAM (Branch Expression Analysis Modeling) presenting 42 differentially expressed genes (DEGs) at different branches (q-value < 1e-4). The central position denotes the start in pseudo-time. Cell fates: the arrow pointing to left indicates cell fate differentiating to vascular tissue, and the arrow pointing to right indicates “procambium (State V)” cell fate.

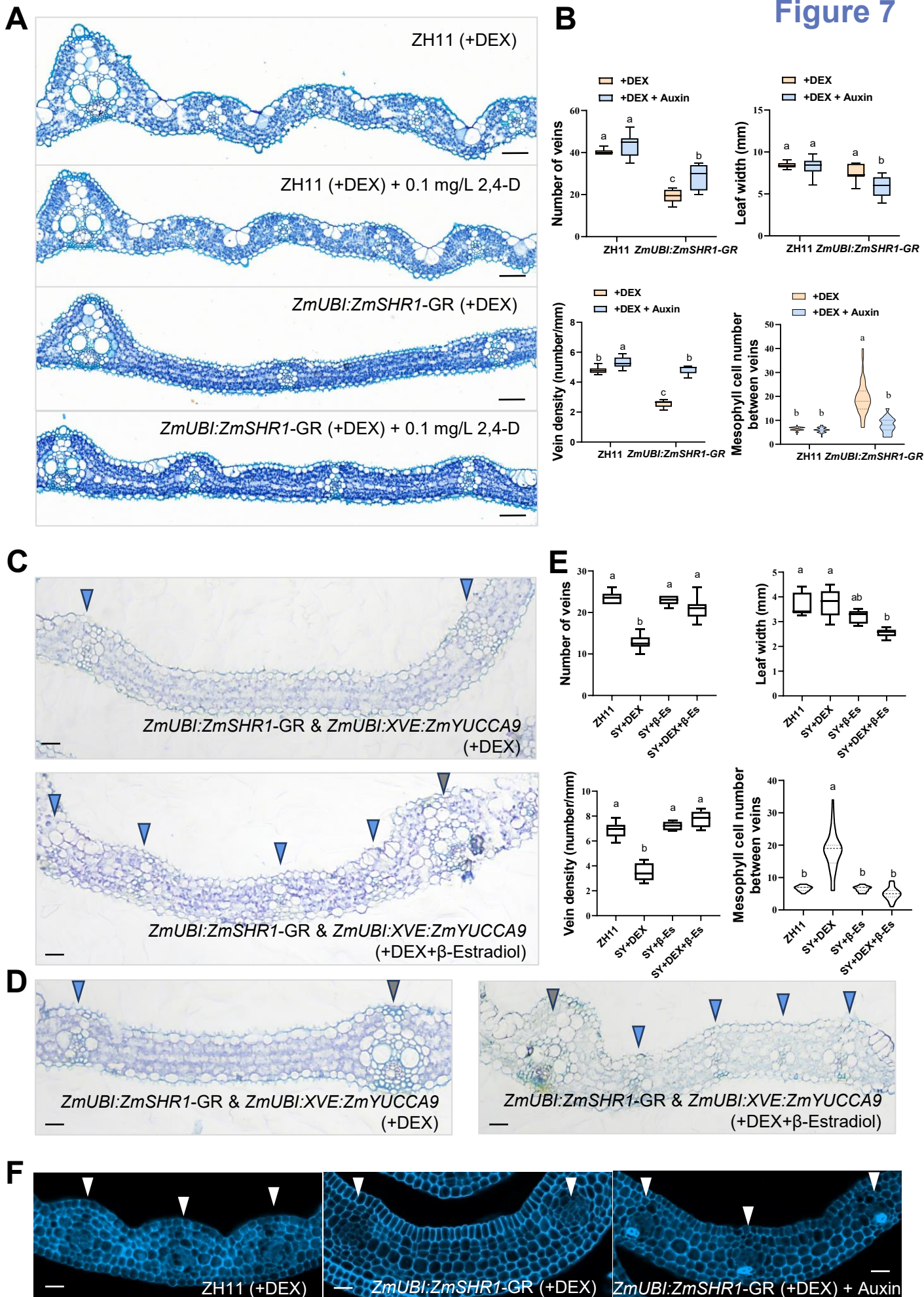
Figure 7

Figure 7. The impact of induced *ZmSHR1* expression and exogenous/endogenous auxin treatment on vein development in rice seedlings.

A. Cross-sectional images of leaf tissues from ZH11 and *ZmUBI:ZmSHR1-GR* rice seedlings under different treatment conditions. The seedlings were subjected to either Dexamethasone (DEX) induction alone, or combined DEX induction and 2,4-D treatment. Two-week-old seedlings began receiving treatments, with regular renewal of treatment reagents. After three weeks of continuous treatment, the middle sections of the newest elongated leaves were collected for paraffin section observation. Scale bar: 50 μ m.

B. Statistical analysis of leaf structural characteristics in ZH11 and *ZmUBI:ZmSHR1-GR* rice seedlings under either DEX induction alone, or combined DEX induction and 2,4-D treatment.

C-D. Leaf cross-sections of *ZmUBI:ZmSHR1-GR* \times *ZmUBI:XVE:ZmYUCCA9* (SY) rice seedlings under different induction conditions. The seedlings were subjected to DEX induction alone or combined DEX and β -estradiol induction. Treatment began on one-week-old seedlings with regular reagent renewal. After three weeks of continuous treatment, the middle sections of the newest elongated leaves were collected for paraffin sectioning. Panels C and D present observations from two independent experimental batches. Grey arrow heads indicate large lateral veins; blue arrow heads indicate small veins. Scale bar: 50 μ m.

E. Quantitative analysis of leaf anatomical features in dual transgenic rice seedlings (*ZmUBI:ZmSHR1-GR* \times *ZmUBI:XVE:ZmYUCCA9*) under either single (DEX) or dual (DEX + β -estradiol) induction conditions.

F. Cross-sections of ZH11 and *ZmUBI:ZmSHR1-GR* rice leaf primordia under either DEX induction alone, or combined DEX induction and 2,4-D treatment. The treatments were started at germination and lasted for 2-3 weeks, after which the middle sections of P3 leaf primordium were sampled for paraffin sectioning and observation of UV activated fluorescent images. White arrow heads indicate the developing veins. Scale bar: 50 μ m.

For (B) and (E), the box, black horizontal line, and whiskers indicate data within interquartile range (IQR, 25th-75th percentiles), the median, lowest and highest value within 1.5 times the IQR, respectively; the data represent means \pm SD and *P* values are calculated using 2-way (B) or 1-way (E) ANOVA with Tukey's HSD test ($n \geq 6$ biological replicates); different letters above the bars indicate significant differences ($P < 0.05$).

Fiaure 8

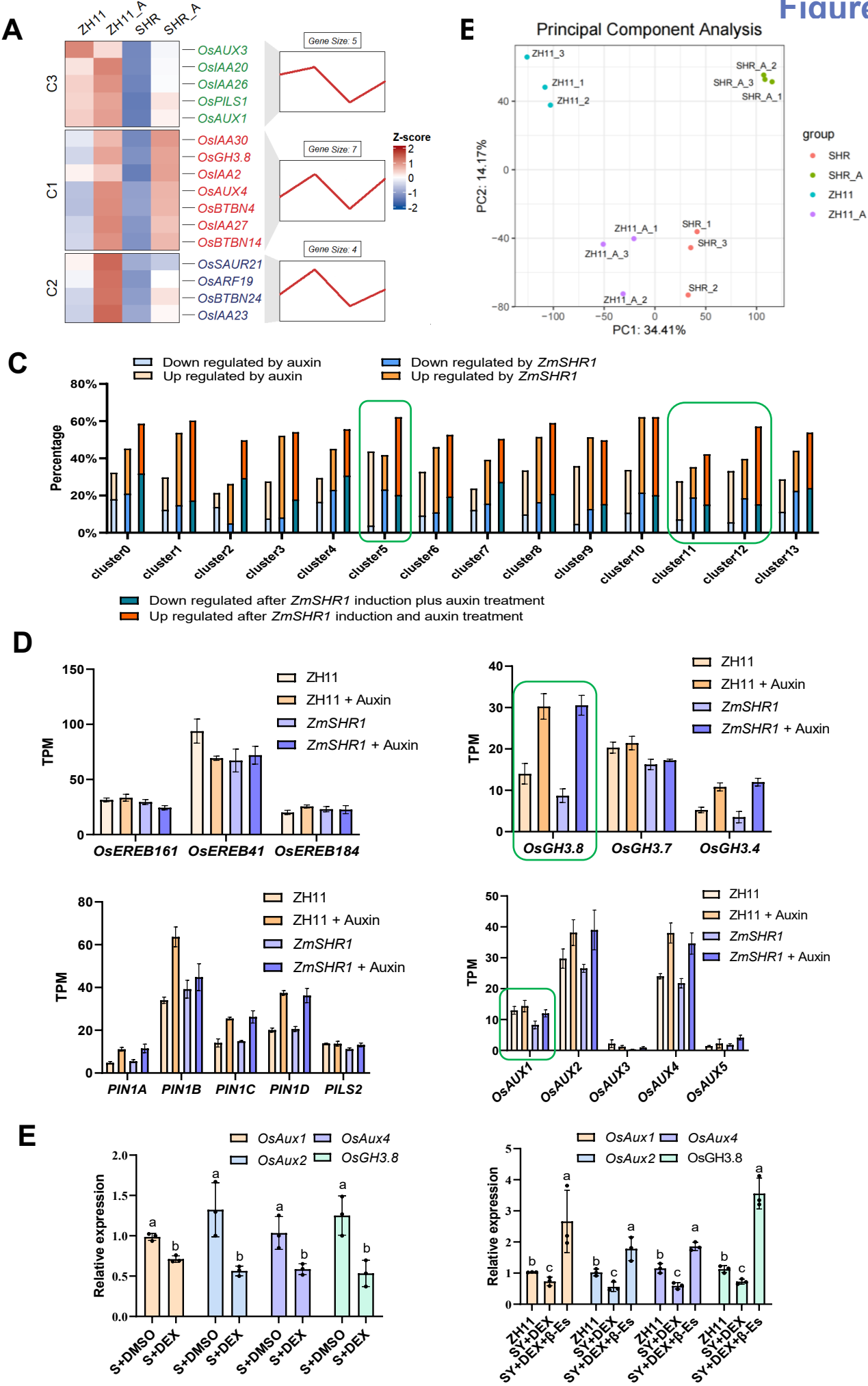


Figure 8. The correspondence of *ZmSHR1* expression / auxin treatment with the expression of rice genes homologous to maize middle ground tissue or procambium enriched genes.

A. The expression pattern analysis of differentially expressed auxin related genes from the transcriptome data of rice leaf primordia, following induced expression of *ZmSHR1* and/or auxin treatment. C1-C3: heatmap of the clusters of DEGs that are downregulated in response to *ZmSHR1* induction and upregulated in response to auxin treatment, obtained using the ClusterGVis package. The right side shows line plots of the expression trend of DEGs in each cluster. ZH11: ZH11 with dexamethasone (DEX) induction; ZH11_A: ZH11 (+DEX) + 0.1 mg/L 2,4-D; SHR: *ZmUBI:ZmSHR1-GR* (+DEX); SHR_A: *ZmUBI:ZmSHR1-GR* (+DEX) + 0.1 mg/L 2,4-D.

B. Principal component analysis (PCA) plot of transcriptome data from rice leaf primordia following induced expression of *ZmSHR1* and/or auxin treatment. The expression matrix was subjected to variance stabilizing transformation (VST) and filtered at the gene level (lowly expressed genes were removed). Each point in the plot represents a sample, with colors indicating different treatment groups.

C. Differential expression patterns of homologous genes in rice leaf primordia transcriptomes under *ZmSHR1* induction and/or auxin treatment. These homologous genes correspond to enriched genes from each of the 14 cell clusters in maize leaf primordia (Figure 3A). The green box highlights cell clusters associated with higher gene numbers of both upregulated rice homologs responsive to auxin treatment and downregulated rice homologs affected by *ZmSHR1* induction.

D. Differential expression of *AtANT1* homologs and auxin-related genes in rice leaf primordia transcriptomes under *ZmSHR1* induction and/or auxin treatment. Top left: *AtANT1* homologs; top right: Indole-3-acetic acid-amido synthetases; bottom left: auxin efflux transporters; bottom right: auxin influx carriers. TPM: Transcripts Per Kilobase Million. Error bars represent mean \pm SD (n=3 biological replicates). The genes marked by green box show clear downregulation by *ZmSHR1* induction while considerable upregulation by either auxin treatment alone or combination of *ZmSHR1* induction and auxin treatment.

E. RT-qPCR validation of the expression of *OsGH3.8* and *OsAUX* genes. Left: effects of 6-hour DEX treatment on the relative transcript levels of target genes in the leaf primordia of one-week-old *ZmUBI:ZmSHR1-GR* rice seedlings. Right: effects of 21 days of DEX induction alone or combined DEX and β -estradiol induction on the relative transcript levels of target genes in the leaf primordia of one-week-old *ZmUBI:ZmSHR1-GR* \times *ZmUBI:XVE:ZmYUCCA9* (SY) rice seedlings. The data represent means \pm SD and *P* values are calculated using an unpaired, two-sided *t* test (left, n=3 biological replicates); different letters above the bars indicate significant differences (*P* < 0.05).

Figure 9

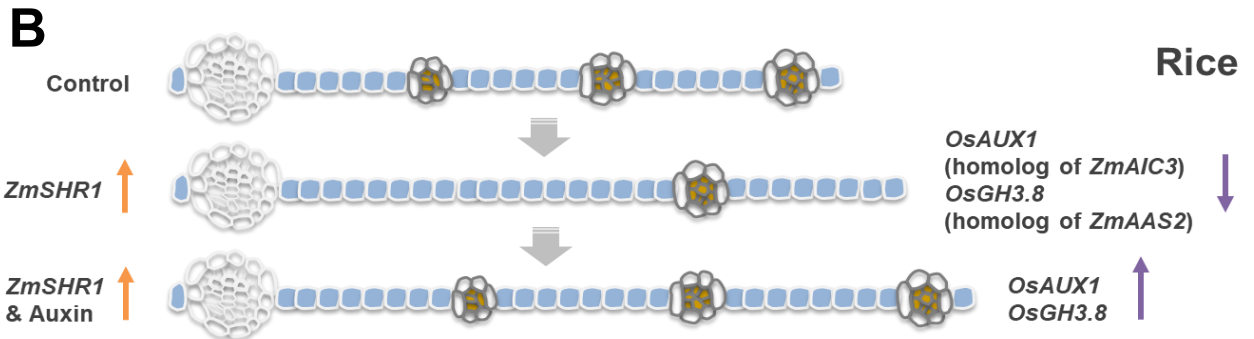
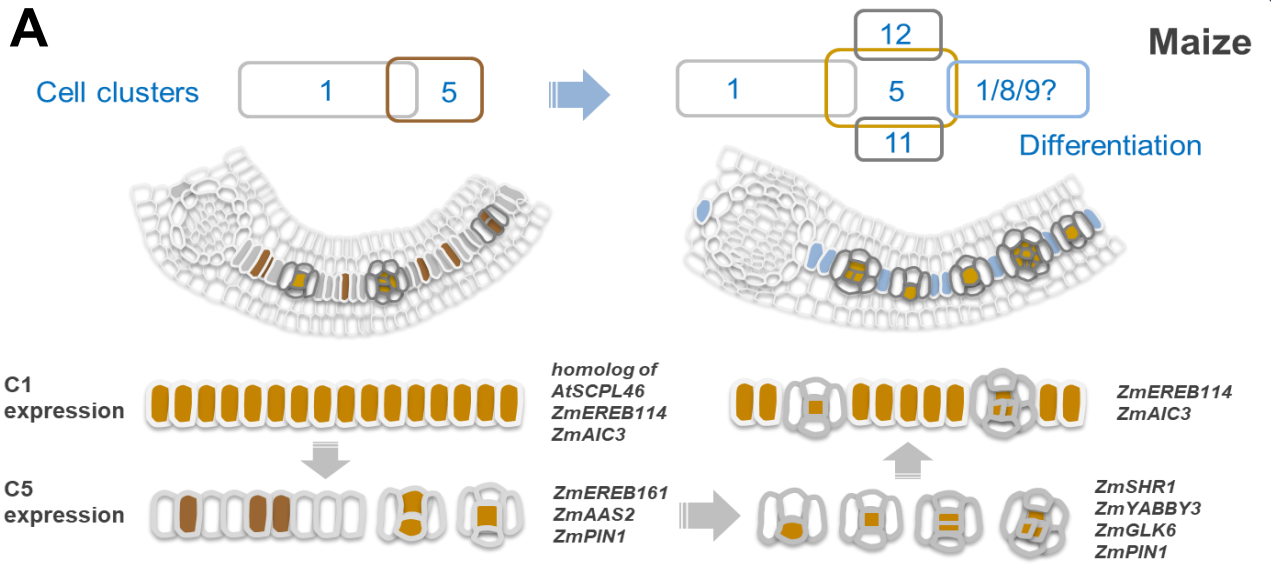
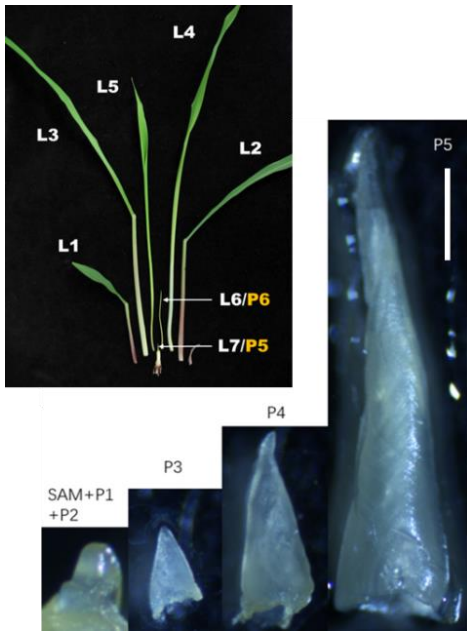


Figure 9. Schematic models combining cell clusters, developmental trajectory, and potential regulators of vein density in maize and rice leaves.

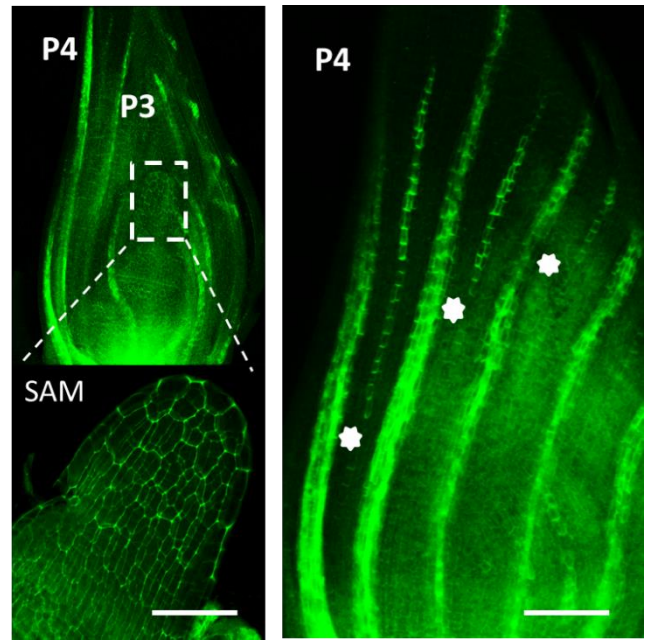
A. Analysis of cellular heterogeneity in the middle ground tissue of maize leaf primordium revealed key cell clusters, such as Cluster 1 and Cluster 5, along with their temporal developmental trajectories. The cell cluster diagrams on the top indicates the differentiation of middle ground tissue (Cluster 1) into middle layer mesophyll cells (Cluster 8 or 9), and procambial cells (Cluster 5) into phloem (Cluster 11) and xylem (Cluster 12) cells. Physical layout of these cell types (as detailed below by the line art of cross sections) was also reflected by the top diagram, with trackable colour code. The differentiation of these cell populations contributes to the dense arrangement of Kranz anatomy. This study uncovered the expression profiles of TFs and auxin related genes including *ZmEREB114*, *ZmAIC3*, *ZmEREB161*, and *ZmAAS2* across the undifferentiated middle layer ground tissue, initiating procambium, and developing vascular bundles. The diagrams at the bottom (sequentially linked by the arrows) further illustrated the spatial-temporal expression of different genes during vascular proliferation and across different developmental stages of the procambia. Brown coloured cells mimic the expression pattern observed by *in situ* hybridization signals.

B. The impact of inducible *ZmSHR1* expression combined with auxin treatment on vein development in rice seedlings. Inducing *ZmSHR1* expression during leaf development resulted in significantly increased interveinal spacing, while auxin treatment alone did not markedly affect the leaf anatomy. However, when auxin treatment is applied simultaneously with *ZmSHR1* induction, it effectively restored the suppressed vein formation by *ZmSHR1* induction (as shown in **Figure 7A, B**). Correspondingly, *OsAUX1* (homolog to *ZmAIC3*) and *OsGH3.8* (homolog to *ZmAAS2*) are the representative rice genes homologous to maize middle ground tissue or procambium enriched genes, which are both downregulated in response to *ZmSHR1* induction and upregulated in response to auxin treatment. What differs between maize (Kranz) and rice (non-Kranz) during vein development may include the number, location or activation state of cells expressing regulatory genes such as *ZmAAS2/OsGH3.8* or *ZmAIC3/OsAUX1*. Active cells for the key step of intermediate vein initiation were identified in maize leaf primordium (deep brown colored single or double cells displayed at the bottom left diagram of **A**), but were currently missing or remained to be further clarified in rice leaf primordium.

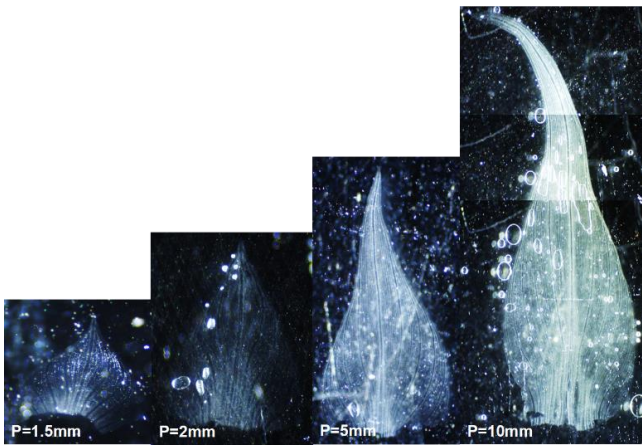
A



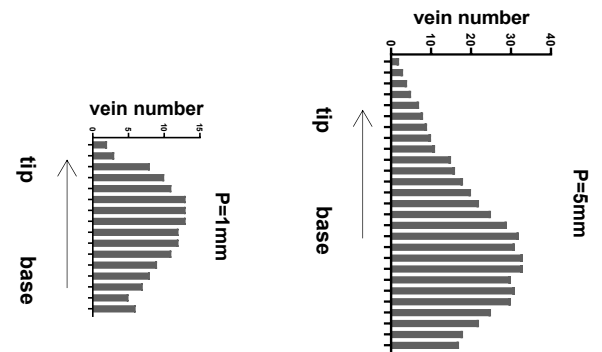
B



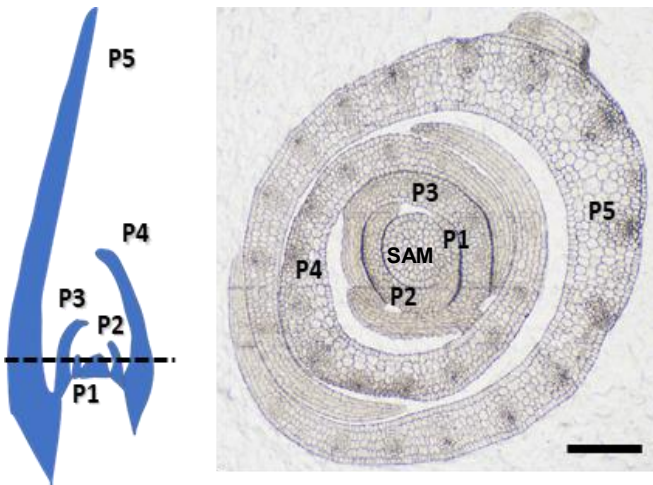
C



D



E



F



Supplemental Figure 1. The growth pattern of leaf primordia.

A. Leaf primordia are initiated at time intervals known as plastochrons (P), such that the youngest primordium (P1) is closest to the SAM, and older primordia (P2, P3, etc.) are consecutively further away. The first leaf to be produced after germination (and hence the oldest) is L1, and subsequent leaves are L2, L3, etc. Each leaf thus has a “P” number to denote relative developmental stage and an “L” number to denote age. Leaf blades are separated from leaf sheath tissue by the ligule, which is established around P5 (Want et al., 2016). The image here shows the visible maize leaves: L1, L2, L3, L4, and L5. L6 is at P6 and L7 is at P5. Dissected leaf primordia are also shown: P1, P2, P3, P4, and P5. Scale bar: 1000 μ m.

B. Confocal image showing pZmPIN1a::ZmPIN1a:YFP fluorescence marked developing veins in maize leaf primodium. Left: SAM plus four most recently initiated leaf primordia (P1-P4). Right: greater magnification of P4, asterisks indicate the leading ends of elongating veins. P, plastochron; SAM, shoot apical meristem. Scale bar: 50 μ m.

C. The maize primodium of 1.5mm, 2.5mm, 5mm and 10mm in size are detached, unrolled, and flattened with the adaxial side facing up (P=1.5mm means the length of primodium is 1.5 mm).

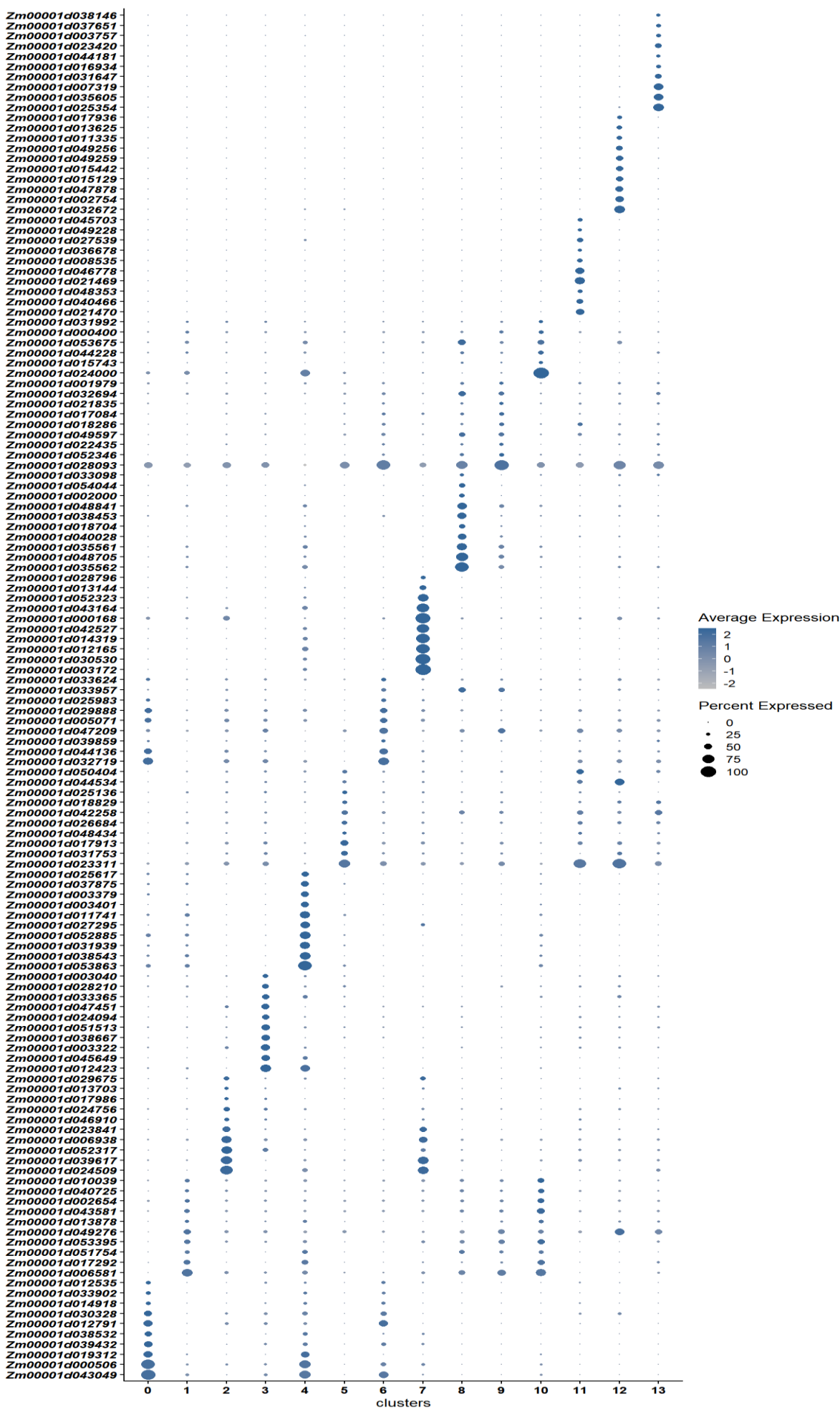
D. Vein number distribution in maize leaf primordia from tip to base. Veins were counted from serial paraffin sections and half of the number from each section were presented in the column charts. The longitudinal length of leaf primordia presented here were 1 mm and 5mm, respectively.

E. Schematic on the left shows the longitudinal section of SAM plus five most recently initiated maize leaf primordia (P1-P5). Dashed line indicates the position of the transverse section shown on the right. Scale bar: 100 μ m.

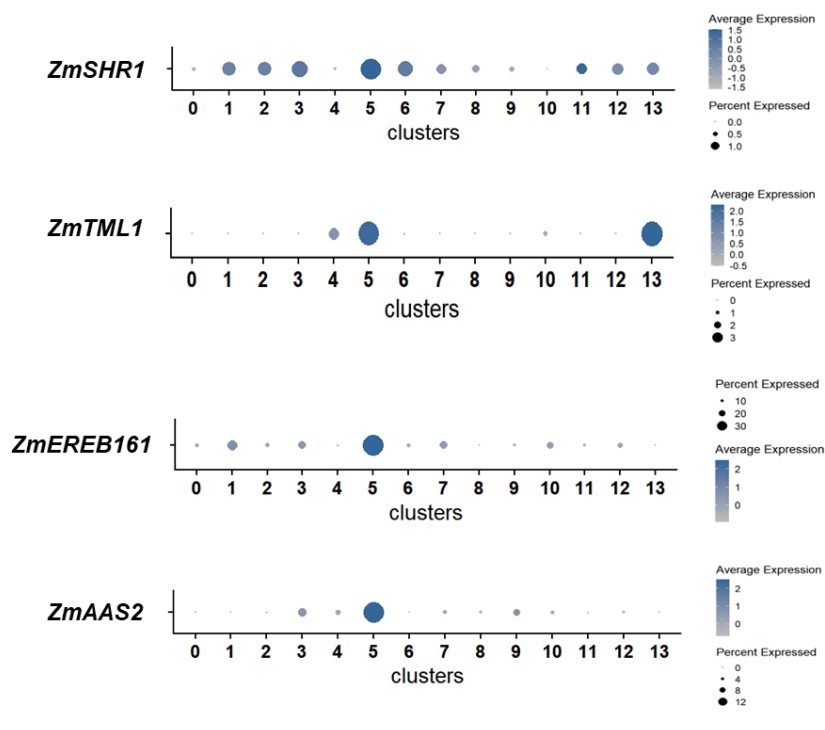
F. Images showing the visible leaves (L1-L3) and dissected leaf primordia (P1-P4) from rice seedlings. Note that P3 and P4 of rice are slimmer than those in maize. Scale bar: 500 μ m.

(Supports Figures 1, 2).

A

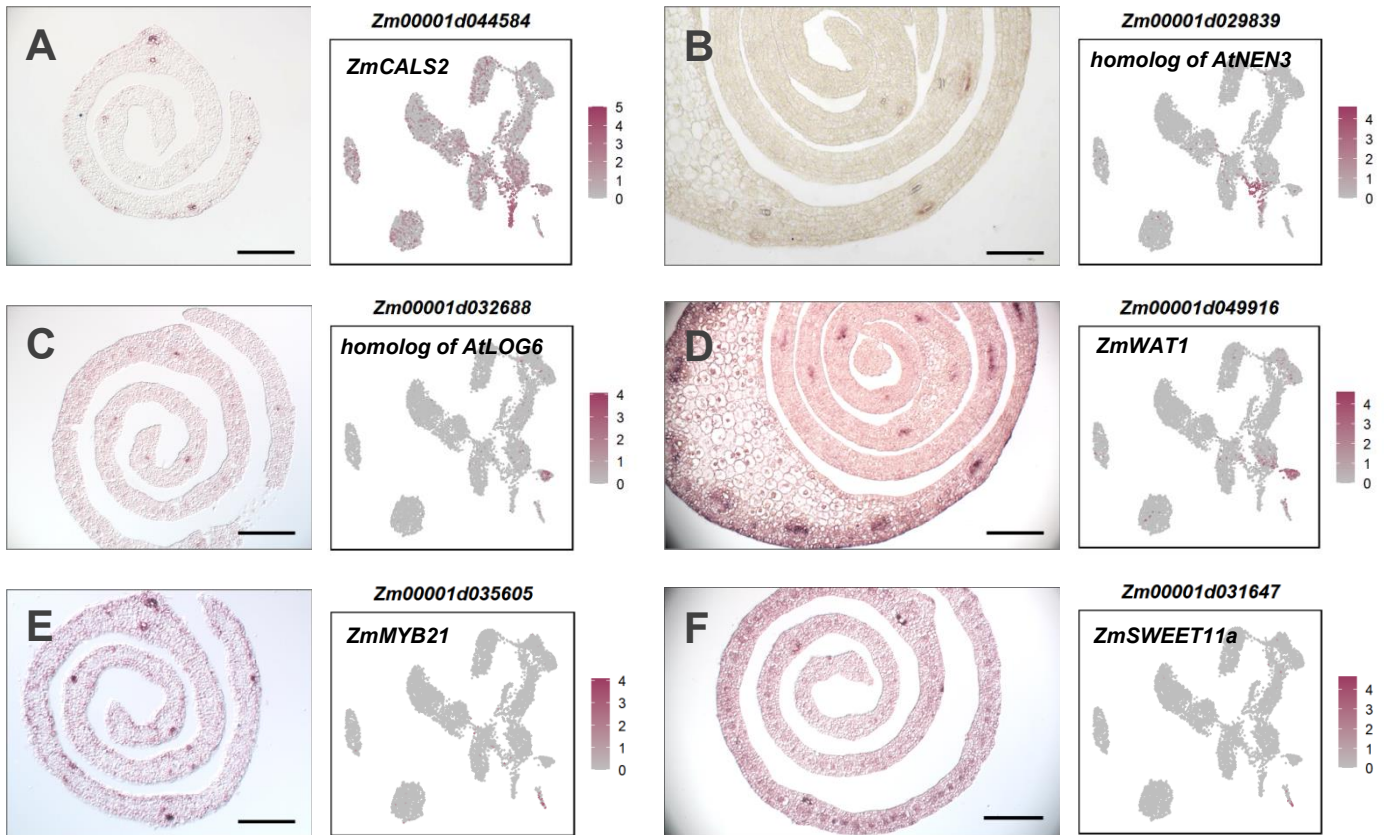


B



Supplemental Figure 2. Dot map showing the top 10 and selected marker genes from each of the different cell clusters. Dot color, the average expression level; Dot size, proportion of cluster cells expressing a given gene. (Supports Figures 3-6).

Supplemental Figure 3



Supplemental Figure 3. *In situ* expression patterns of representative marker genes from xylem and phloem related cell clusters.

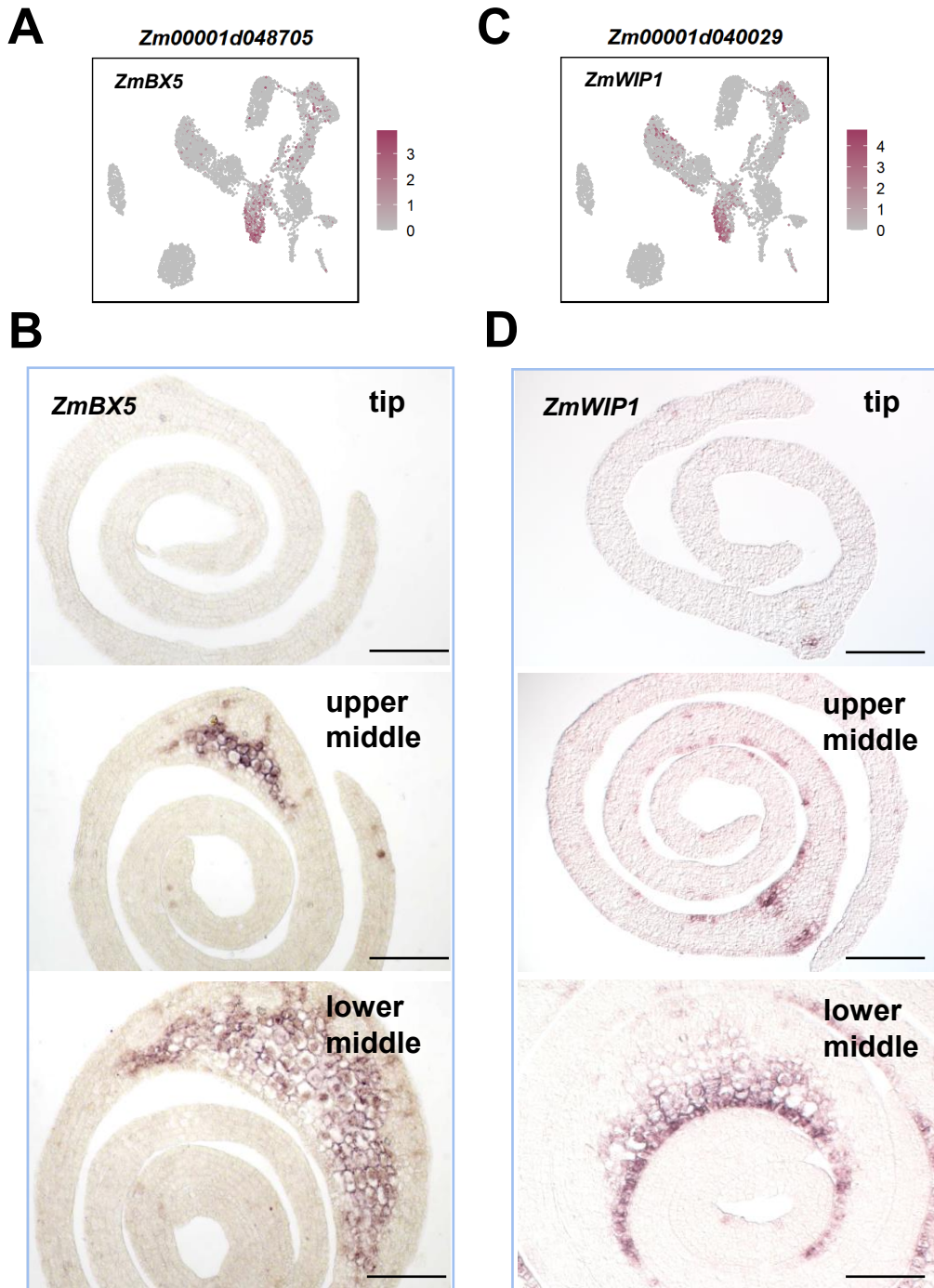
A and B. *In situ* hybridization and UMAP plots for the expression patterns of Cluster 11 (phloem related)-enriched genes.

C and D. *In situ* hybridization and UMAP plots for the expression patterns of Cluster 12 (xylem related)-enriched genes.

E and F. *In situ* hybridization and UMAP plots for the expression patterns of Cluster 13-enriched genes.

Names of the cluster-enriched genes are indicated above the figures. Scale bar: 100 μ m. (Supports Figure 3).

Supplemental Figure 4



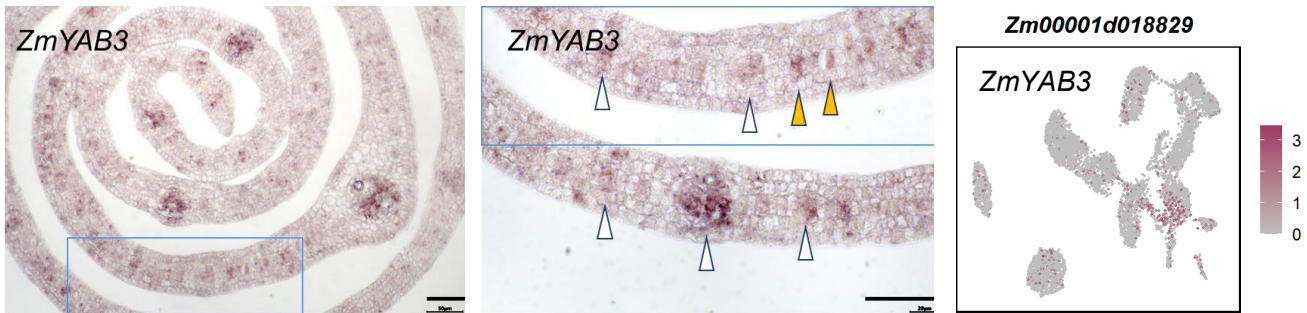
Supplemental Figure 4. *In situ* expression patterns of representative marker genes from mesophyll and parenchymal cell related clusters.

A and C. Expression pattern of Cluster 8-enriched genes by UMAP plots.

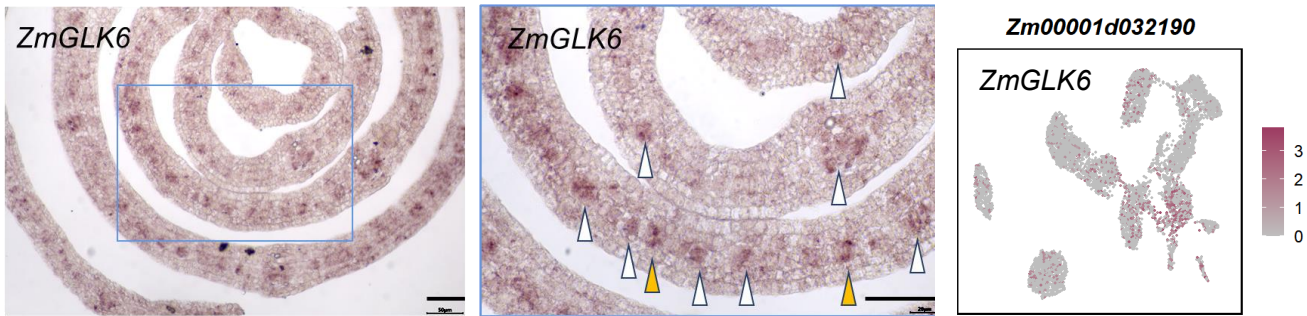
B and D. *In situ* hybridization for the expression patterns of Cluster 8-enriched genes on transverse sections of maize leaf primordia. Scale bar: 120 μ m.

(Supports Figure 3).

A

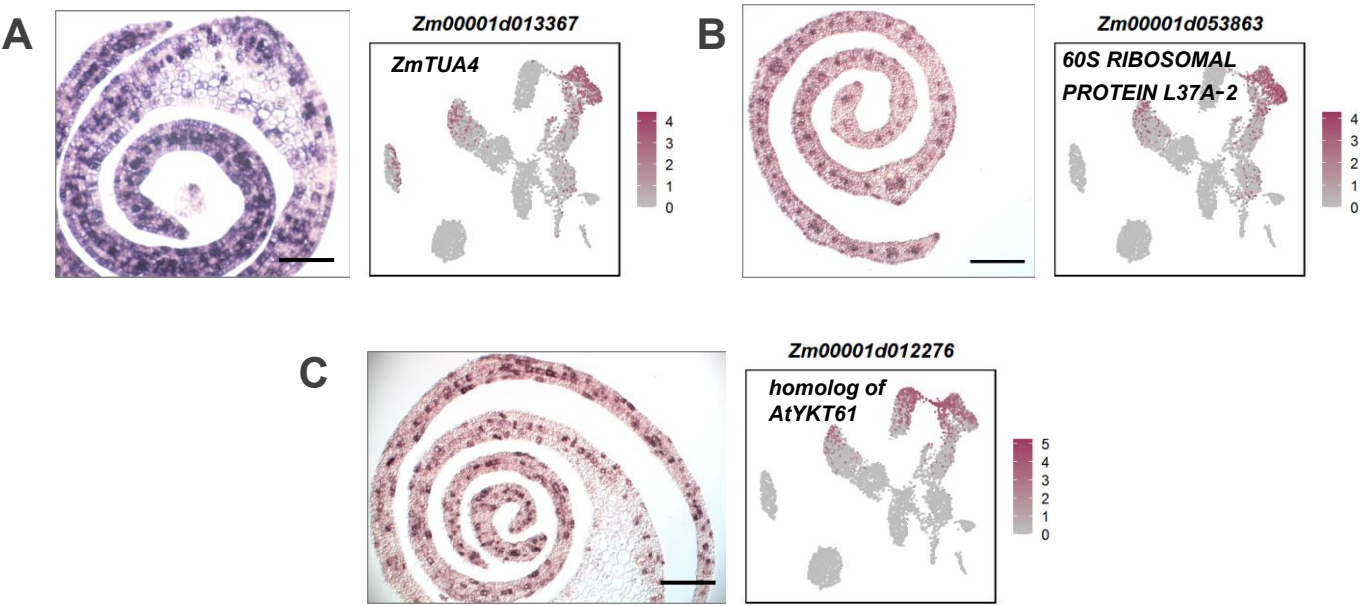


B



Supplemental Figure 5. The expression patterns of *ZmYAB3* and *ZmGLK6*.

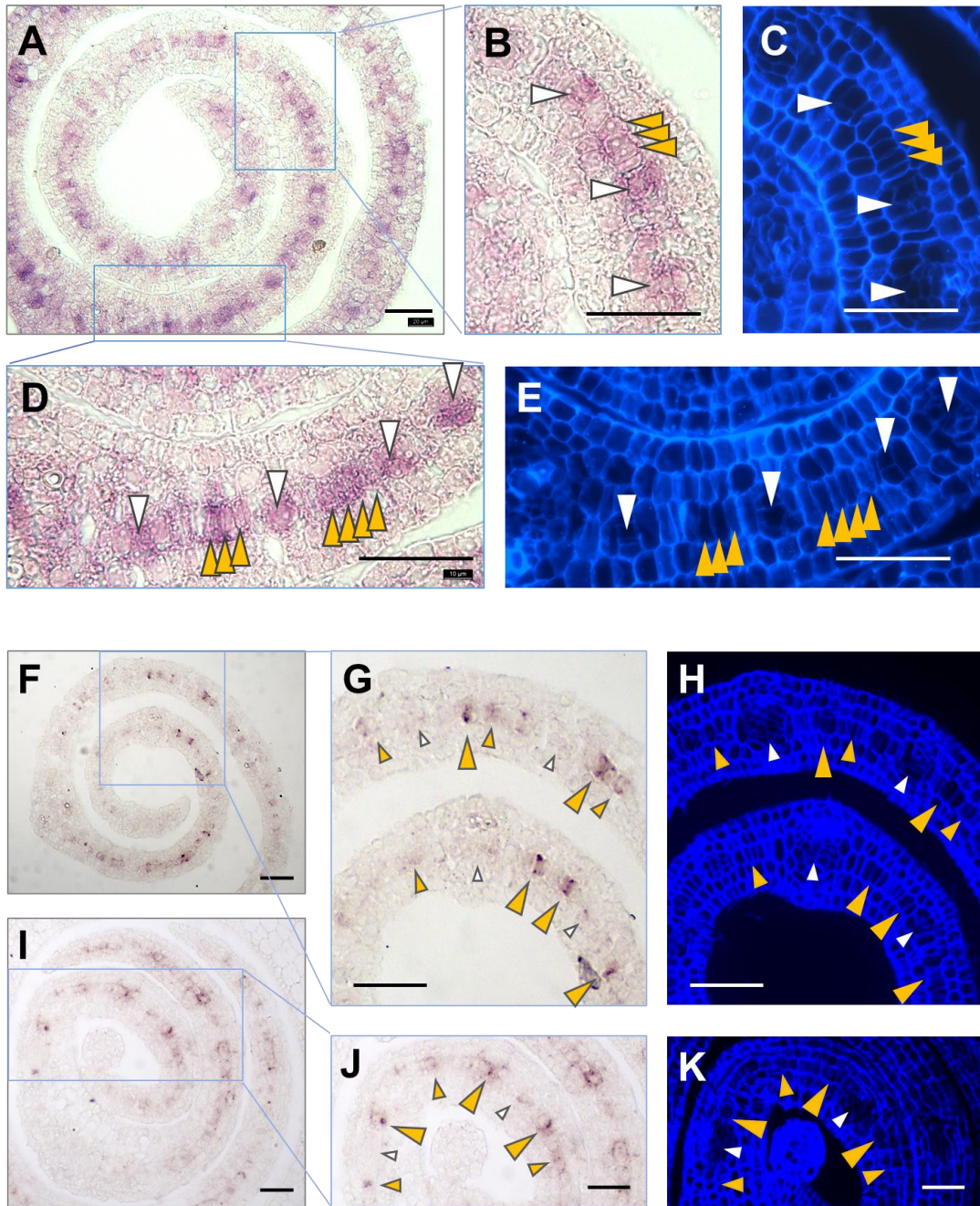
Left column, *in situ* hybridization for the transcript localization of *ZmYAB3* (A) and *ZmGLK6* (B) on transverse sections of maize leaf primordia. Middle column, close-up images of the blue square framed regions from left column. Right column, expression pattern of selected genes by UMAP plots. Scale bar: 50 μ m. White arrows indicate the differentiating procambium; orange arrows indicate the potential single procambial initial cell. (Supports Figure 3).

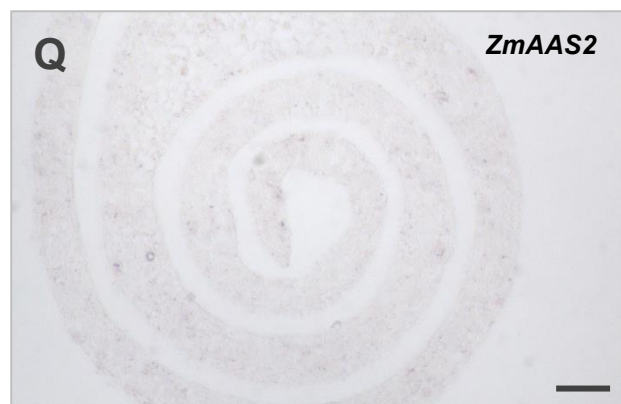
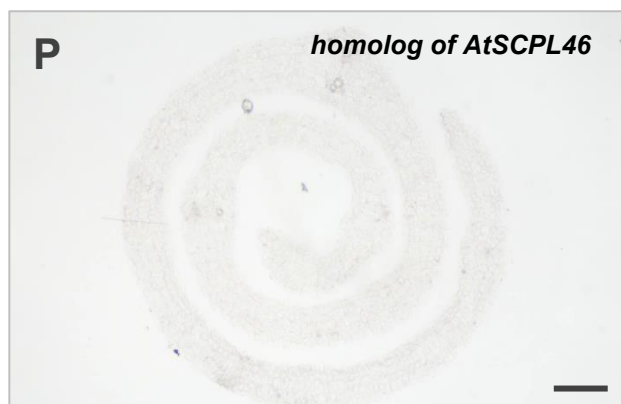
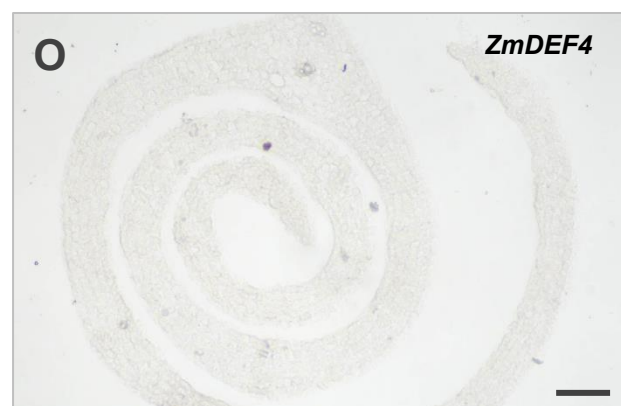
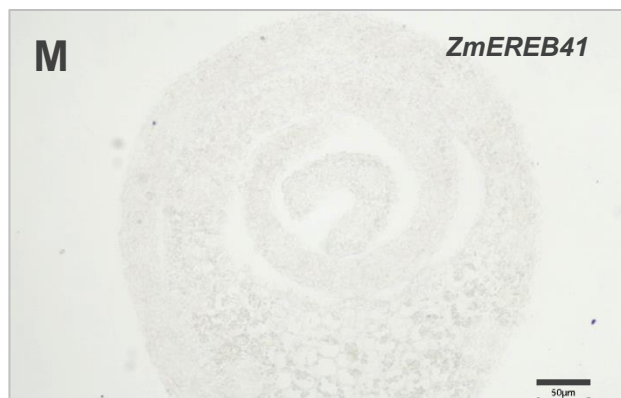


Supplemental Figure 6. *In situ* expression patterns of representative marker genes related with Clusters 1 and 4.

A-C show *in situ* hybridization and UMAP plots for the expression patterns of Clusters 0, 1, 3 and 4-enriched genes. Scale bar: 100 μ m. (Supports Figure 3).

Supplemental Figure 7





Supplemental Figure 7. Localization of *ZmEREB114* and *ZmEREB41* transcripts in the middle cell layer of maize leaf primordium, and hybridization results with sense RNA probes.

A. *In situ* hybridization showing the distribution of *ZmEREB114* transcript in the middle section of P4 leaf primordia. Scale bar: 40 µm.

B and D. Magnified images of the blue square framed regions from (A), showing *ZmEREB114* signals at different cell types of early Kranz anatomy; **C and E.** UV activated fluorescent images of the corresponding regions from (B) and (D). Scale bar: 40 µm.

F and I. *In situ* hybridization showing the distribution of *ZmEREB41* transcript in the middle section of P4 leaf primordia. Scale bar: 40 µm.

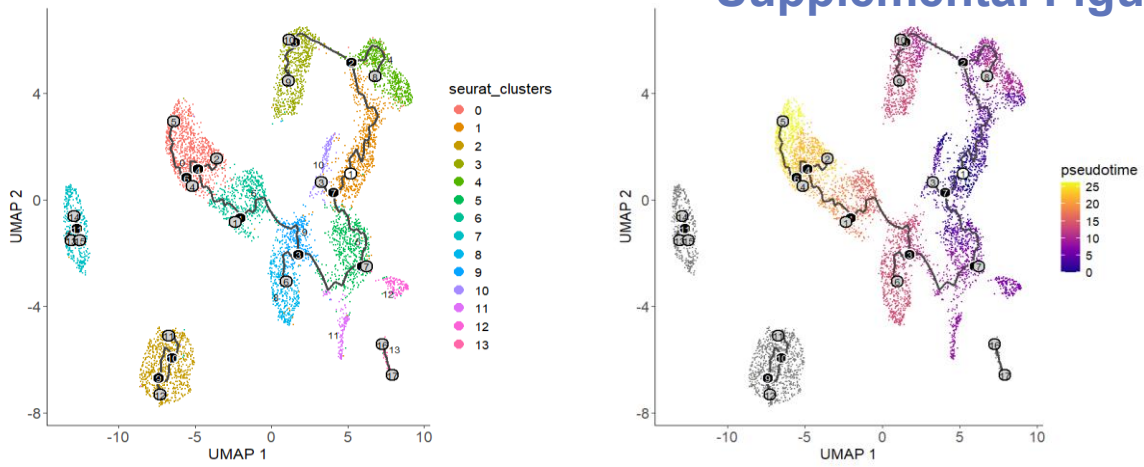
G and J. Magnified images of the blue square framed regions from (F) and (I), showing *ZmEREB41* signals at different cell types of early Kranz anatomy; **H and K.** UV activated fluorescent images of the corresponding regions from (G) and (J). Scale bar: 40 µm.

White arrow heads indicate the differentiating or differentiated procambium (including early differentiating ones with the primary adaxial and abaxial precursors of BS cells, generated by the 1st and 2nd periclinal divisions of a single procambial initial cell); orange arrow heads indicate the potential procambial initial cells (indicated by *in situ* hybridization signals) prior to periclinal division. Smaller sized arrows indicate less strong *in situ* hybridization signals.

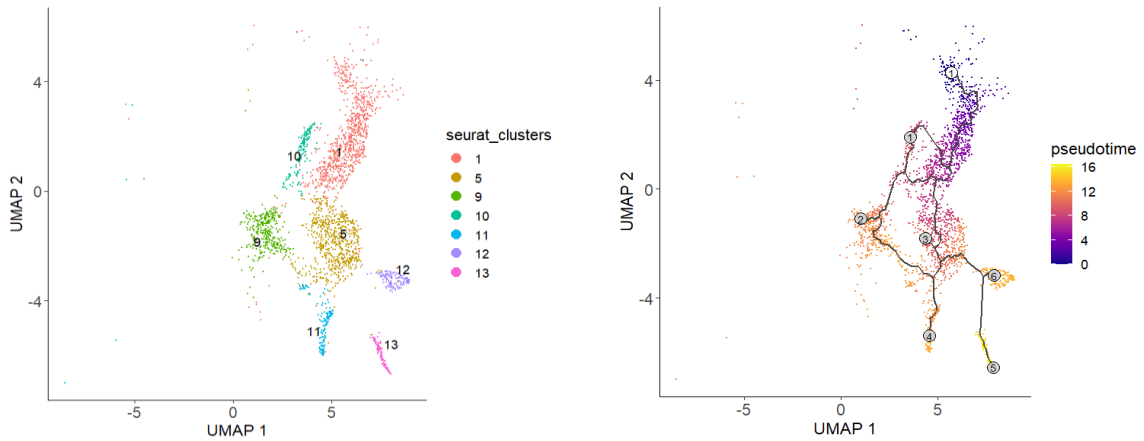
L-Q. *In situ* hybridization results with sense RNA probes of *ZmEREB114*, *ZmEREB41*, as well as other genes from **Figure 4** and **6**. No specific signals were detected. Scale bar: 50 µm. (Supports Figure 5).

Supplemental Figure 8

A

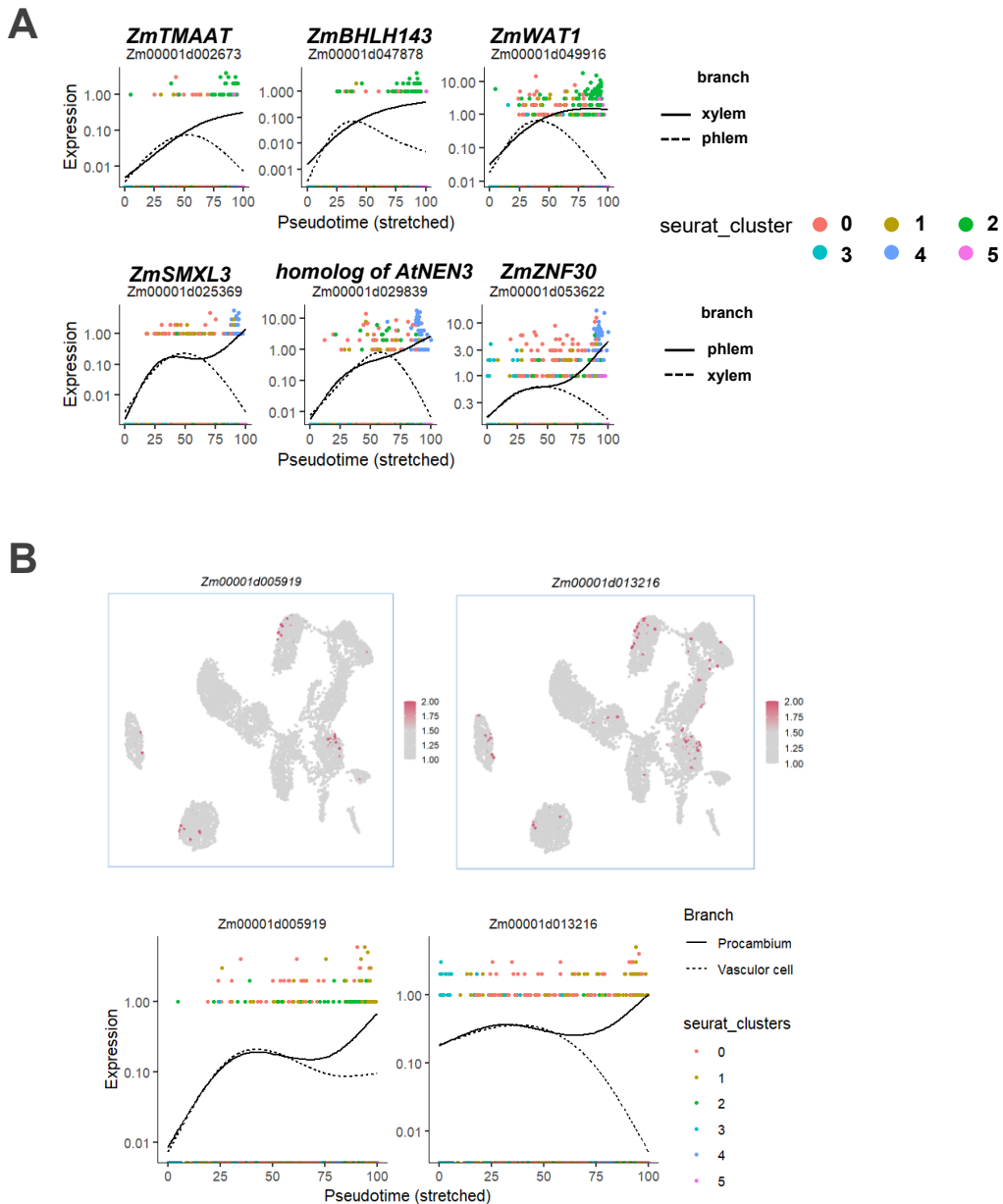


B



Supplemental Figure 8. Differentiation trajectory in a P4 maize primodium.

The successive differentiation trajectory of the whole **(A)** and a subset **(B)** of the 14 cell clusters over pseudo-time generated by “Monocle 3”. Dots, individual cells; cell clusters are coloured differently and labelled with numbers (refer to the circled numbers in **Figure 3A**). The white colour circled number “1” on Cluster 1 indicates the beginning of the pseudo-time. Colour gradient on the right represents increasing pseudo-time from beginning to end. The grey colour circled numbers represent different branches along the pseudo-time trajectory, and the black colour circled numbers indicated the points where cell fate differentiates. (Supports Figure 6).



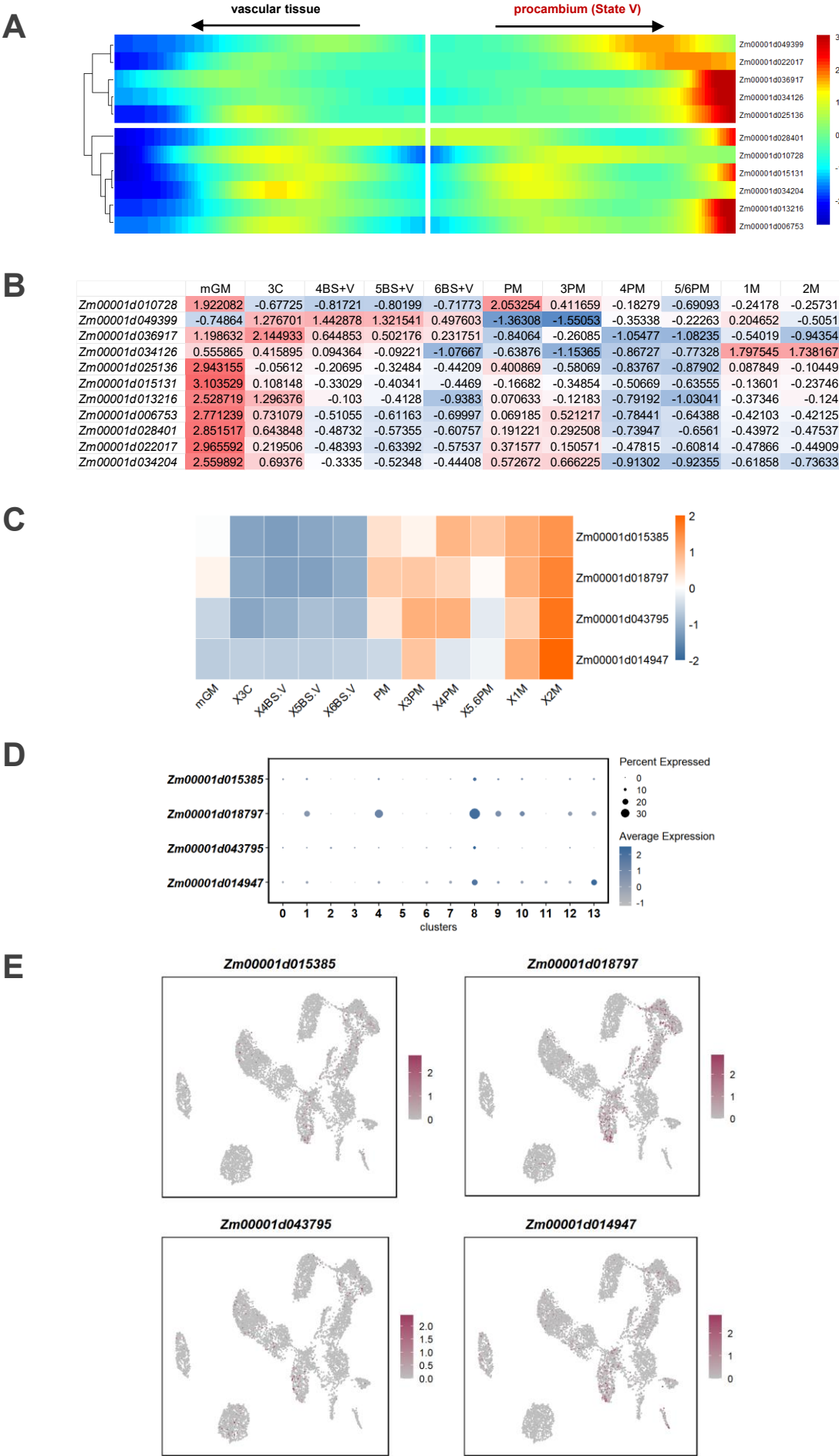
Supplemental Figure 9. Expression trends of xylem, phloem, and procambium marker genes along the pseudo-temporal trajectory.

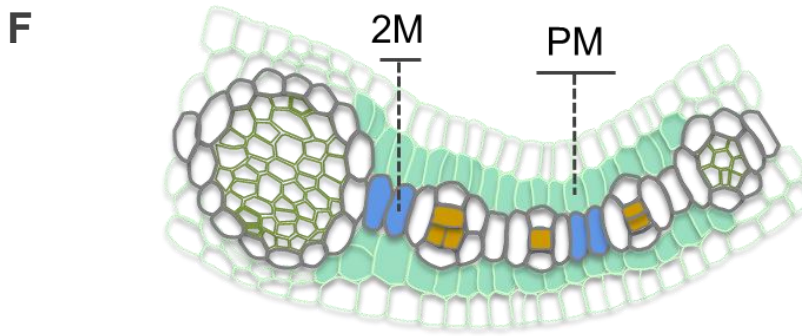
A. Kinetics plot showing relative expression of xylem (upper panel) and phloem (lower panel) marker genes along developmental pseudo-time splitting at “branch point 2”.

B. UMAP plots (upper panel) and kinetics plot showing relative expression of “State V” genes along developmental pseudo-time splitting at “branch point 1” (lower panel).

The abscissa represents the quasi-chronological order, and the ordinate represents the relative expression value of genes. The line denotes the smoothed average expression. The colored dots on the top shows the major cluster of contributing cells to the expression. (Supports Figure 6).

Supplemental Figure 10





Supplemental Figure 10. Cell fate and differential gene expression analysis along pseudo-time, and cross-reference from the LCM data.

A. Heatmap depicting expression patterns of enriched genes in cells assigned to differentiation state V along the pseudo-time development trajectory. The central position denotes the start in pseudo-time. Cell fates: the arrow pointing to left indicates cell fate differentiating to vascular tissue, and the arrow pointing to right indicates “procambium (State V)” cell fate.

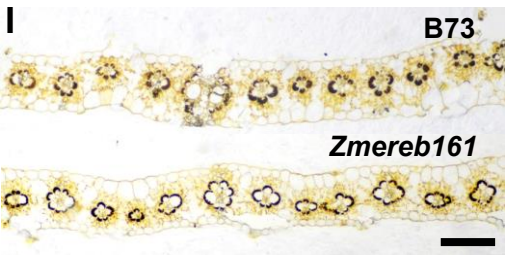
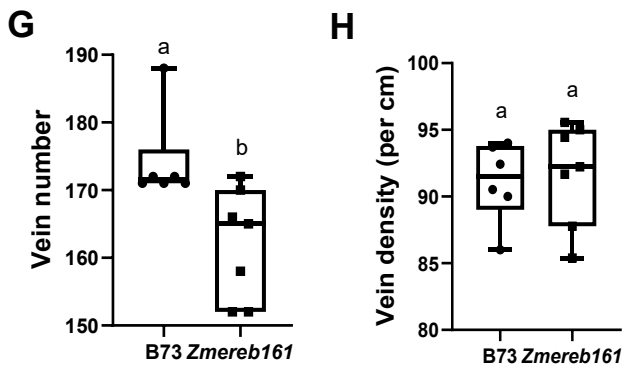
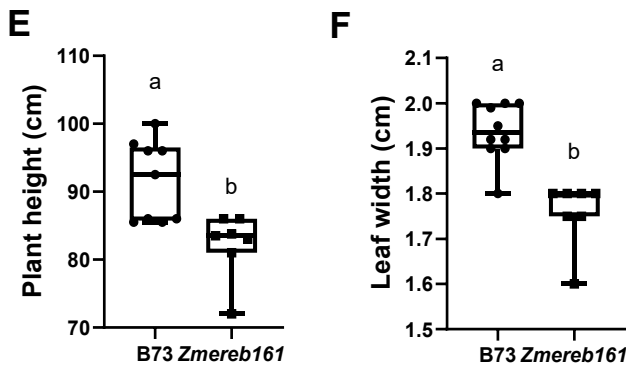
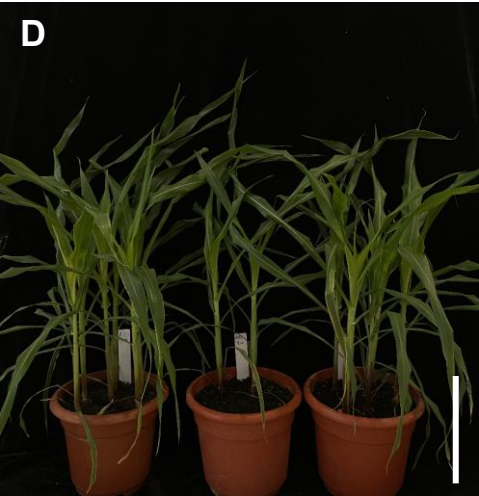
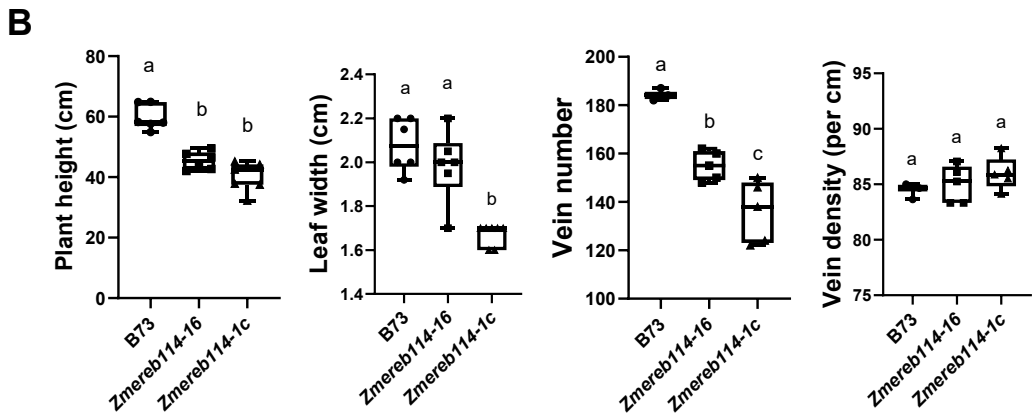
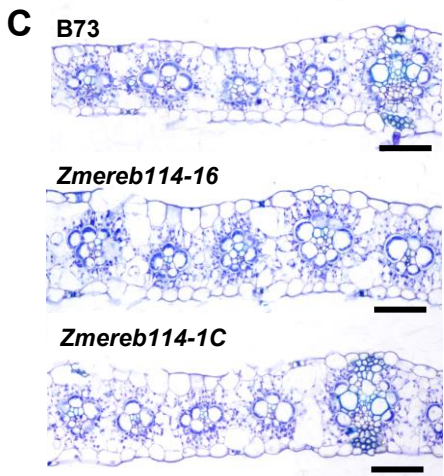
B. Cell type-specific enrichment patterns for genes highlighted in panel (A), cross-referenced with the cell type annotations reported in Liu et al., 2022.

C-E. “2M” samples from the LCM data assisted further annotation of mesophyll cell clusters for the snRNAseq data. Heat maps showing the selected “2M” cell enriched genes (C); Dot plots (D) and UMAP plots (E) showing the “Cluster 8” enrichment of the selected genes. Dot colour, proportion of cluster cells expressing a given gene; Dot size, the average expression level.

F. Schematics of the anatomy and cell types representing the upper middle section of P4 leaf primordium. “2M” and “PM” cells described in Liu et al. (2022) were filled in blue and light green colours respectively.

(Supports Figures 3 and 6).

Supplemental Figure 11



Supplemental Figure 11. Characterization of maize *zmereb114* and *zmereb161* mutants.

A. The phenotype of maize wild-type (B73) and *zmereb114* mutant plants at approximately 15 days of growth. Scale bar: 10 cm.

B. Quantification of plant growth and leaf vascular traits of B73 and *zmereb114* mutants. Boxplots show plant height (n = 6, 6, 7 biological replicates, respectively), leaf width (n = 6, 6, 7 biological replicates, respectively), vein number (n = 3, 5, 5 biological replicates, respectively), and vein density (n = 3, 5, 5 biological replicates, respectively) of B73, *zmereb114-16*, and *zmereb114-1c*, in the middle sections of the 2nd fully expended leaves from the top of 4-weeks-old plants.

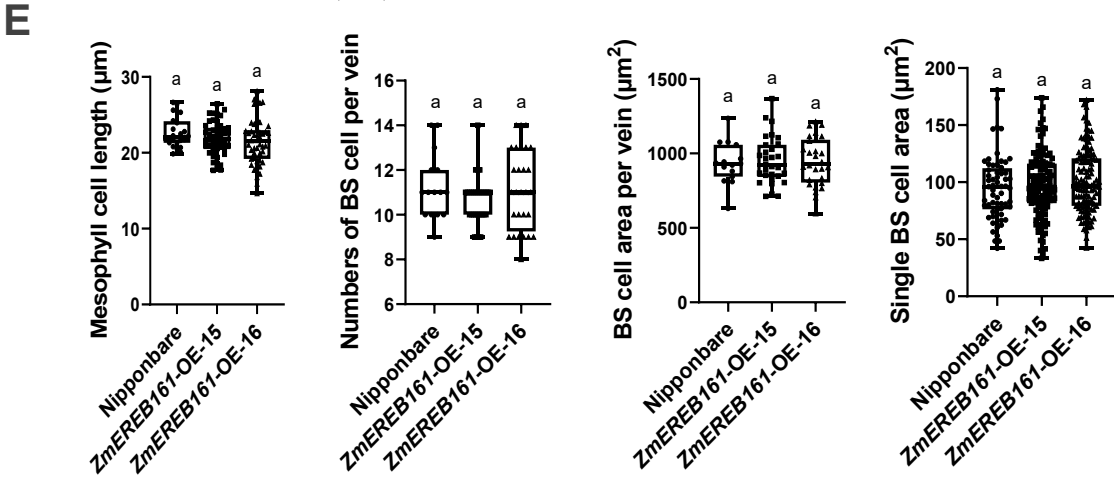
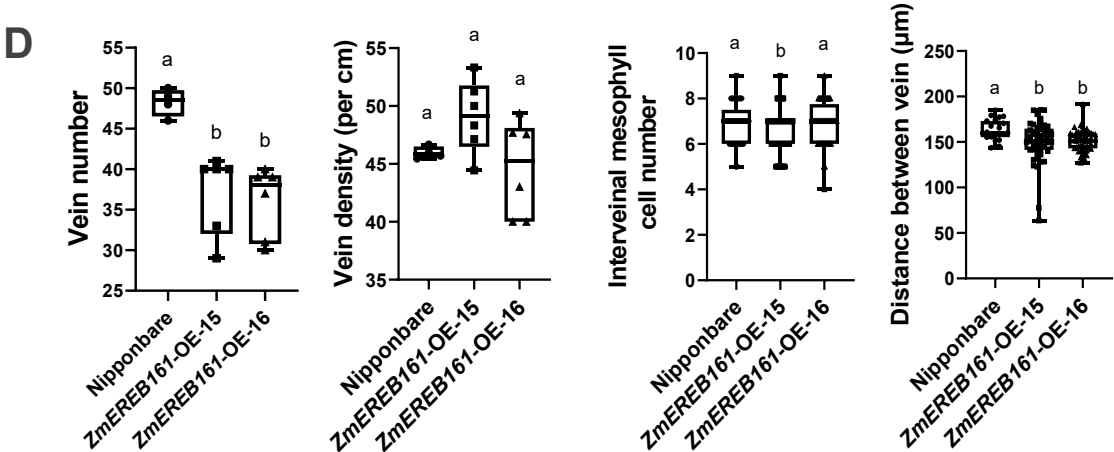
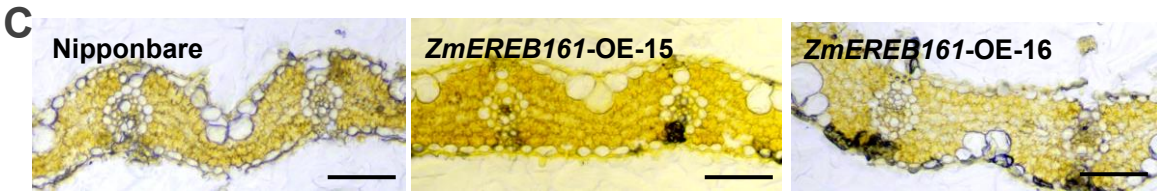
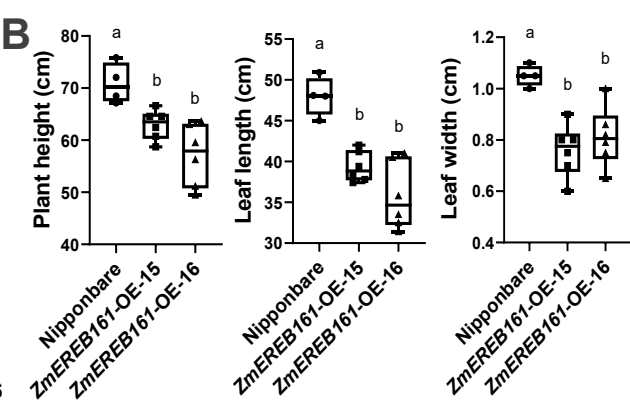
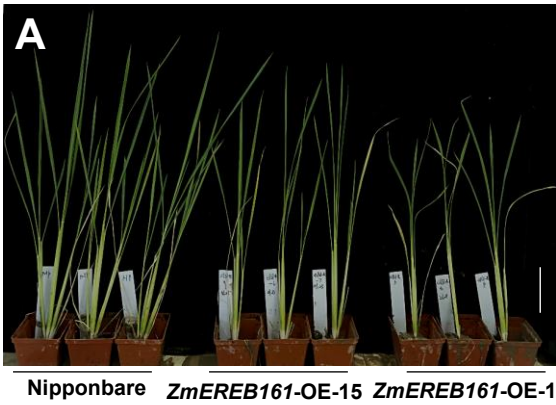
C. Transverse sections of B73 and *zmereb114* mutant plants with toluidine blue staining. Scale bar: 80 μ m.

D. The phenotype of maize wild-type (B73) and *zmereb161* mutant plants. Scale bar: 23 cm.

E-H. Quantification of plant growth and leaf vascular traits of B73 and *zmereb161* mutants. Boxplots show plant height (n = 9, 7 biological replicates, respectively) (E), leaf length (n = 6, 7 biological replicates, respectively) (F), vein number (n = 10, 7 biological replicates, respectively) (G), and vein density (n = 6, 7 biological replicates, respectively) (H) of B73 and *zmereb161* mutant, in the middle sections of the 2nd fully expended leaves from the top of 4-weeks-old plants.

I. Starch staining of transverse sections of leaves from B73 and *zmereb161* mutant to assist in displaying vein arrangement. Scale bar: 120 μ m.

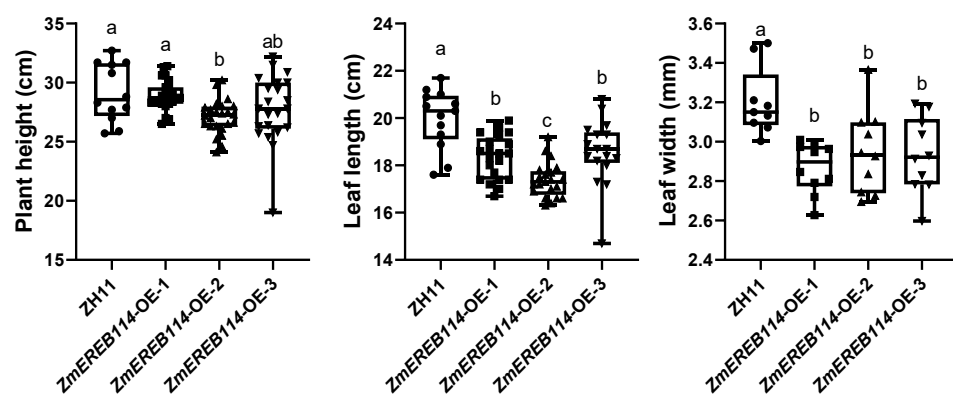
The box, black horizontal line, and whiskers indicate data within interquartile range (IQR, 25th-75th percentiles), the median, lowest and highest value within 1.5 times the IQR, respectively; the data represent means \pm SD and *P* values are calculated using 1-way ANOVA with Tukey's HSD test (C, n \geq 3 biological replicates) or an unpaired, two-sided *t* test (E-H, n \geq 6 biological replicates) ; different letters above the bars indicate significant differences (*P* < 0.05). (Supports Figure 5).



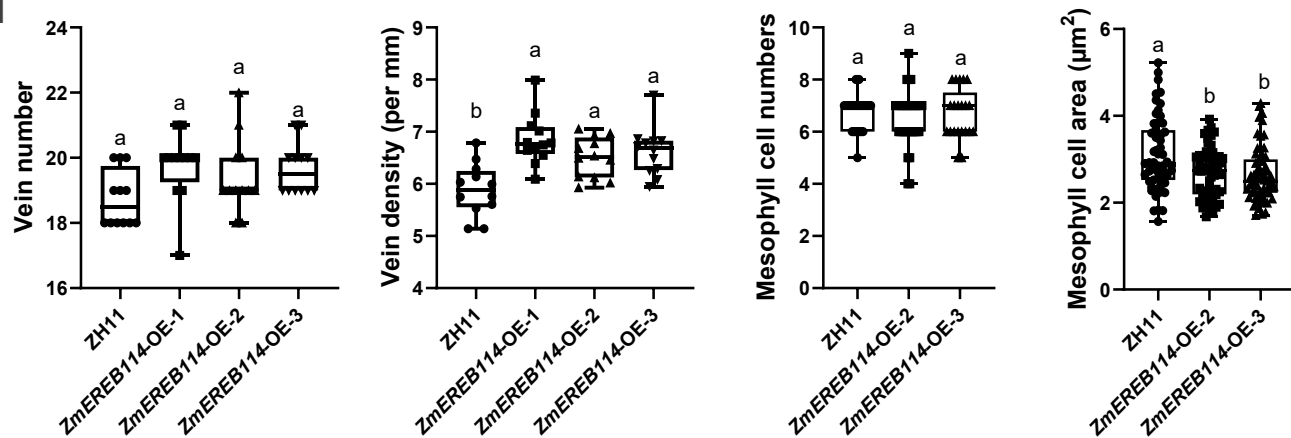
F



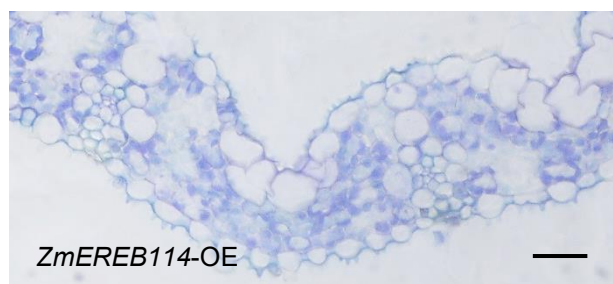
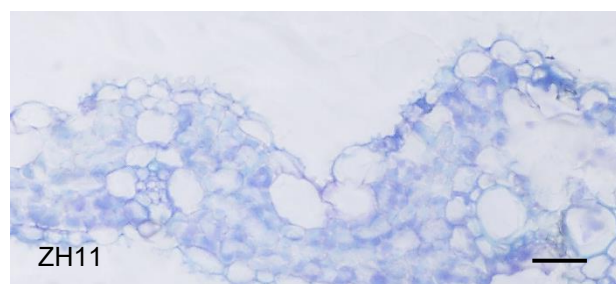
G



H



I



Supplemental Figure 12. Characterization of *ZmUBIpro::ZmEREB161* and *ZmUBIpro::ZmEREB114* transgenic rice plants.

A. The phenotype of rice wild-type (Nipponbare) and *ZmUBIpro::ZmEREB161* transgenic plants at approximately 30 days of growth. Scale bar: 10 cm.

B. Quantification of plant growth of Nipponbare and *ZmUBIpro::ZmEREB161* transgenic plants. Boxplots show plant height (n = 4, 6, 6 biological replicates, respectively), leaf length (n = 4, 6, 6 biological replicates, respectively), and leaf width (n = 4, 6, 6 biological replicates, respectively), measured in the middle sections of the 2nd fully expended leaves from the top of 6-weeks-old T1 plants.

C. Starch staining of transverse sections of Nipponbare and *ZmUBIpro::ZmEREB161* transgenic plants to assist in displaying leaf anatomy. Scale bar: 60 μ m.

D-E. Quantification of leaf anatomy traits of Nipponbare and *ZmUBIpro::ZmEREB161* transgenic plants. Boxplots show vein, mesophyll cell and bundle sheath cell related parameters measured in the middle sections of the 2nd fully expended leaves from the top of 6-weeks-old T1 plants.

(D) The vein number (n = 4, 6, 6 biological replicates, respectively), vein density (n = 4, 6, 6 biological replicates, respectively), number of mesophyll cells between two vascular bundles (n = 69, 88, 105 biological replicates, respectively), and the distance between two vascular bundles (n = 23, 48, 47 biological replicates, respectively). (E) The mesophyll cell length (n = 24, 48, 47 biological replicates, respectively), average number of bundle sheath cells surrounding each vascular bundle (n = 15, 30, 28 biological replicates, respectively), average area of bundle sheath cells surrounding each vascular bundle (n = 15, 30, 28 biological replicates, respectively), and area of single bundle sheath cells in the middle layer (n = 60, 120, 112 biological replicates, respectively).

F. The phenotype of rice wild-type (ZH11) and *ZmUBIpro::ZmEREB114* transgenic plants at approximately 14 days of growth. Scale bar: 5 cm.

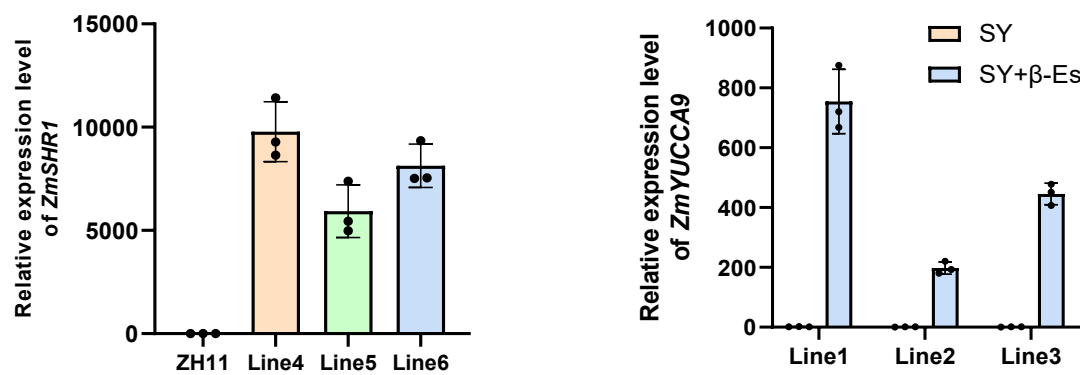
G. Quantification of plant growth of ZH11 and *ZmUBIpro::ZmEREB114* transgenic plants. Boxplots show plant height, leaf length, and leaf width, measured in the middle sections of the 2nd fully expended leaves from the top of 2-weeks-old T1 plants (n >= 9).

H. Quantification of leaf anatomy traits of ZH11 and *ZmUBIpro::ZmEREB114* transgenic plants. Boxplots show vein and mesophyll cell related parameters measured in the middle sections of the 2nd fully expended leaves from the top of 2-weeks-old T1 plants (n >= 12).

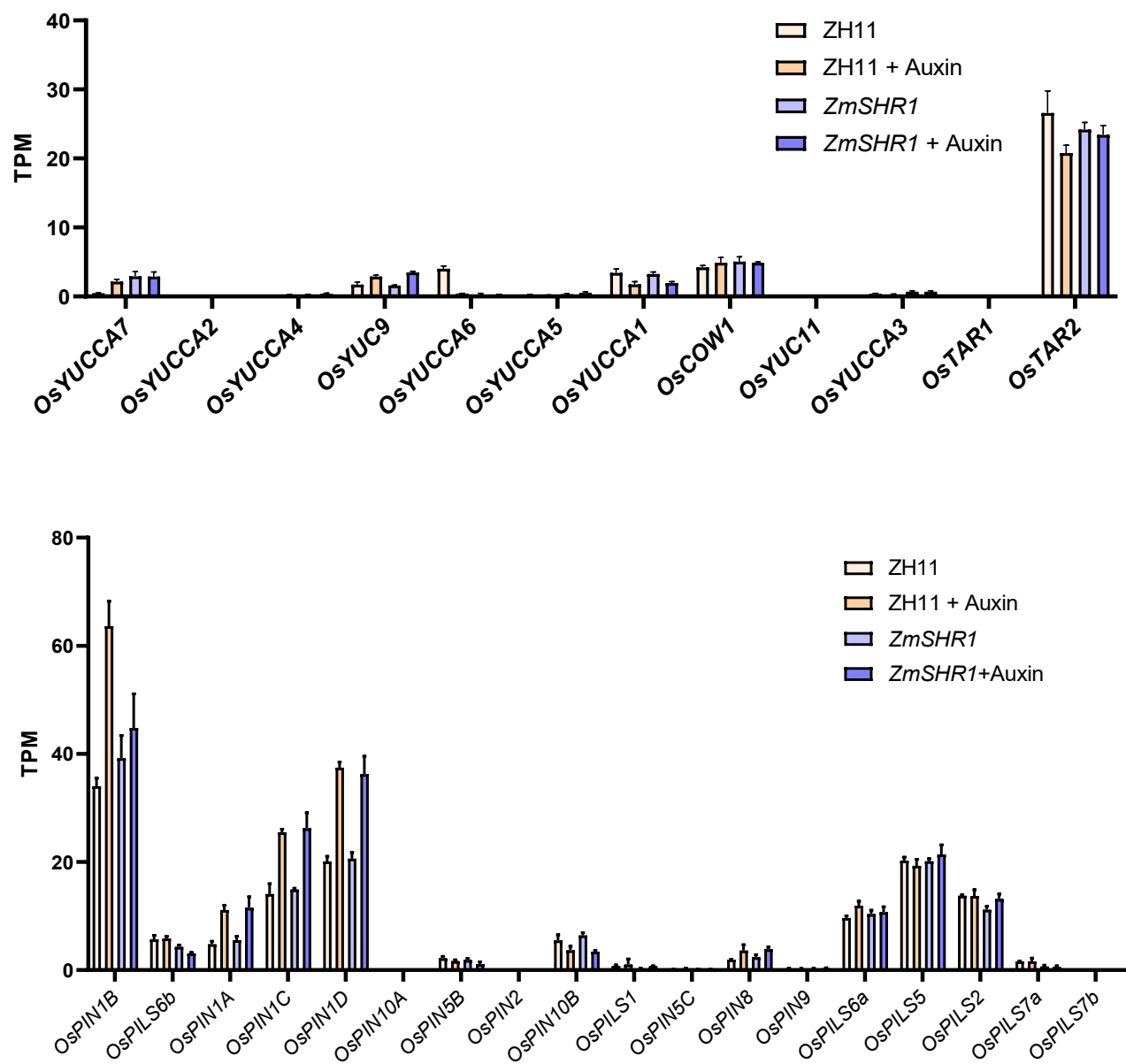
I. Transverse sections of ZH11 and *ZmUBIpro::ZmEREB114* transgenic plants with toluidine blue staining. Scale bar: 20 μ m.

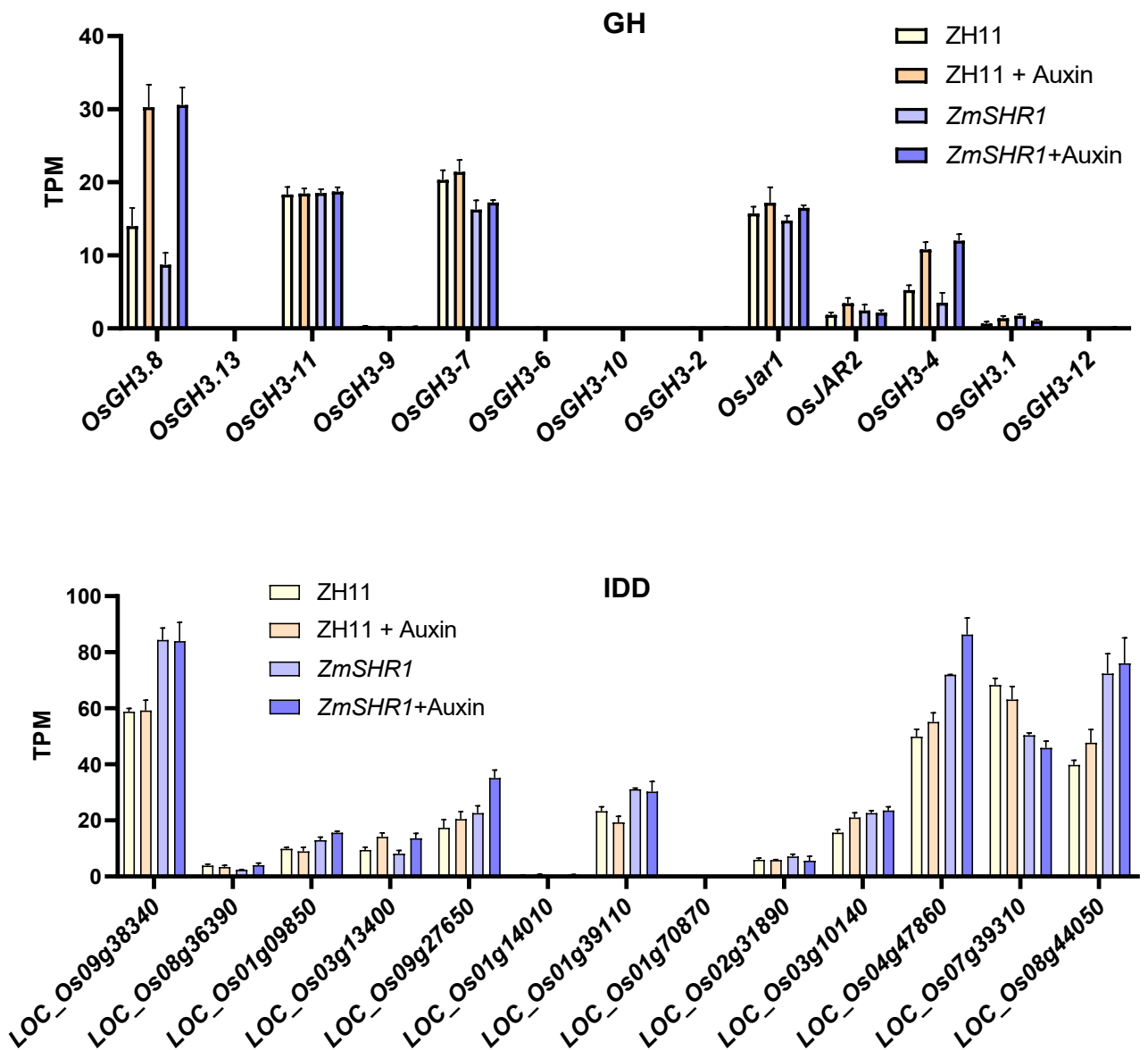
The box, black horizontal line, and whiskers indicate data within interquartile range (IQR, 25th-75th percentiles), the median, lowest and highest value within 1.5 times the IQR, respectively; the data represent means \pm SD and *P* values are calculated using 1-way ANOVA with Tukey's HSD test (n>=4 biological replicates); different letters above the bars indicate significant differences (*P* < 0.05). (Supports Figure 5).

A



B





Supplemental Figure 13. The impact of induced *ZmSHR1* expression and auxin treatment on the expression of auxin-related or IDD genes in rice leaf primordia.

A. The relative transcript levels of *ZmSHR1* in the leaves of *ZmUBI:ZmSHR1-GR*, and of *ZmYUCCA9* in the leaves of *ZmUBI:ZmSHR1-GR* × *ZmUBI:XVE:ZmYUCCA9* (SY) transgenic lines. Error bars represent mean ± SD (n=3 biological replicates).

B. ZH11 and *ZmUBI:ZmSHR1-GR* rice leaf primordia under either Dexamethasone (DEX) induction alone or combined DEX induction and 2,4-D treatment. Treatment began on two-week-old seedlings with regular reagent renewal. After three weeks of continuous treatment, the leaf primordium (up to P3) were sampled for transcriptome sequencing and data analysis. Error bars represent mean ± SD (n=3 biological replicates). TPM: Transcripts Per Kilobase Million.

(Supports Figure 8).